THE MONTE CARLO METHOD

Chapter 7

7-1 INTRODUCTION

In the treatment of deterministic computational methods contained in the foregoing chapters, the computing errors are systematic. Aside from uncertainties in the cross section data, they arise not only from the discretization of the time-space-angle-energy phase space for numerical computation but also from the fact that the present state of the art does not, with rare exception, permit the full representation of three-dimensional configurations in deterministic transport computations. Hence the errors introduced by representing three-dimensional configurations by simplified one- or two-dimensional models are of paramount importance, and much of the effort in deterministic methods development is directed toward the related problems of computer memory, time, and accuracy encountered in extending deterministic methods to treat large multidimensional problems.

In contrast, Monte Carlo methods now in existence are capable of treating very complex three-dimensional configurations.[1-10] Moreover, the continuous treatment of energy, as well as space and angle, obviates discretization errors such as result, for example, from the use of multigroup approximations. Hence for a given set of cross section data, the errors in Monte Carlo calculations take the form of stochastic uncertainties. Before examining their properties, however, we must first outline the procedure one goes through in carrying out a Monte Carlo calculation.

In its simplest form, Monte Carlo consists of simulating a finite number, say N, of particle histories through the use of a random number, or, more correctly, pseudo random number generator.[5, 11] In each particle history random numbers are generated and used to sample appropriate probability distributions for scattering angles, track length distances between collisions, and so on. For simplicity we consider here a fixed source problem in a nonmultiplying medium with only capture and elastic scattering. Assuming that the problem is time-independent, each history is begun by sampling the source distribution to determine the particle's initial energy, position, and

direction. After stochastically determining the number of mean free paths the particle will travel before colliding, the material region and point of collision are determined. By sampling cross section data, it is determined with which nuclide the particle has collided and whether the collision is a capture or a scattering reaction. If it is capture, the history is terminated, but if it is scattering, the distribution of scattering angles must be sampled to give a new direction. Then, in the case of elastic scattering, a new energy is determined by conservation of energy and momentum. With the energy, position, and direction after the collision thus specified the foregoing procedure is repeated for successive collisions until the particle is absorbed or escapes from the system.

Suppose the purpose of the particle tracking is to calculate the expectation or mean value $\bar{x}$ of some quantity. This might be a flux, current, escape probability, or any number of other quantities. Our estimate of such a quantity would then take the form of the mean of N samples,

$$\hat{x} = \frac{1}{N} \sum_{n=1}^{N} x_n, \tag{7-1}$$

where x_n is the contribution of the nth history to that quantity. Thus as the Monte Carlo calculation proceeds, we tally the x_n due to each history in order to calculate the estimated or sample mean $\hat{x}$ at the end of the calculation. When fluxes or similar quantities are of interest, $\hat{x}$ typically is given in terms of the number of collisions, the total track length distance traveled, or other properties related to the individual histories.

The question immediately arises as to how good an estimate our sample value $\hat{x}$ is to the true mean value $\bar{x}$. As seen in Section 7-4, the uncertainty in $\hat{x}$ decreases with increasing numbers of histories, in most cases in asymptotic proportion to $N^{-1/2}$. Moreover, for a fixed number N of histories, estimates with the least uncertainty are most often obtained for quantities to which all or at least a substantial fraction of the histories contribute. Hence the average flux over the entire problem domain is a relatively easy quantity to estimate, since every—or nearly every—particle history contributes to it. On the other hand, the fraction of particles penetrating a thick shield is much more difficult to calculate with any precision. For example, if the shield provides an attenuation of 10^6, then only about one of each million histories contributes to the result! Such quantities, to which only very exceptional histories contribute, can still be calculated successfully using Monte Carlo techniques. This is possible, however, only when the strict analog simulation of particle histories de-

E.E. Lewis & W.F. Miller, Jr.
Computational Methods of Neutron Transport
ANS, 1993

scribed above is abandoned in favor of more powerful stochastic methods that serve to reduce the uncertainty in one or a few quantities. Variance reduction techniques by which this is accomplished are discussed in Section 7-6.

The foregoing discussion directs us back toward the comparison of Monte Carlo and deterministic methods. For unlike deterministic methods stochastic methods can be extended in a relatively straightforward manner to complex three-dimensional configurations. On the other hand, they are of relatively less value when one requires the detailed distribution of a dependent variable, such as spatial profiles of flux or power, even when relatively simple one- or two-dimensional geometries are involved. The reason for this may be viewed as follows. In Monte Carlo, the flux or other quantities are normally not calculated at a point. Rather they are estimated from the number of collisons, particle track lengths, or some other quantity in some incremental volume $\Delta V \Delta \hat{\Omega} \Delta E$ of phase space. Hence if one wanted a detailed spatial distribution of the scalar flux, the domain of the problem would have to be divided in many small ΔV and the flux estimated in each of these cells. However, as the ΔV are taken smaller to improve the spatial resolution of the results, the fraction of the N histories contributing to the flux in any one cell decreases rapidly. Accordingly, the statistical uncertainty in the result may grow rapidly to unacceptable levels, even when a large number of histories is used. While it is often possible to use powerful stochastic techniques to reduce this uncertainty when only one or a few quantities are being estimated, this is usually not the case when comprehensive information is required about the details of the particle distribution. Thus Monte Carlo calculations may not be as appropriate as deterministic methods in these cases.

In the preceding paragraphs, an effort has been made to sketch qualitatively some of the properties of Monte Carlo methods. In what follows we examine the method in more detail by first reviewing the necessary probability distribution laws and then formulating the particle simulation and standard tally procedures for analog Monte Carlo. The estimate of error and the role of variance and the central limit theorem are then discussed. Nonanalog or variance reduction methods for fixed source problems are then discussed.

For clarity, each of these topics is introduced within the context of monoenergetic transport in a simple one-region solid. For once they are understood, it is relatively straightforward to incorporate the energy variable, and the discussion of the spatial tracking of particles through complex multiregion systems falls more naturally into place. We then conclude the chapter with a discussion of criticality calculations using the Monte Carlo Method.

7-2 PROBABILITY DISTRIBUTION FUNCTIONS

In this section we first examine probability distribution functions of one random variable[4, 12] and examine techniques for sampling the resulting distribution. We then examine probability distributions in two variables in order to discuss independence and conditional probabilities.

Functions of a Single Random Variable

We introduce probability distributions by first considering a random variable x. By random variable we mean a variable that takes on particular values with a frequency that is determined by some underlying probability distribution. In our considerations, x is typically some property of a particle history, such as a flight distance, scattering angle, or escape probability, that may take on a range of values. We define

$$P\{a \le x \le b\} = \text{probability that } x \text{ will have a value between } a \text{ and } b$$

There are two functions that are essential to Monte Carlo calculations. These are the probability density function and the cumulative probability distribution, sometimes referred to simply as the distribution function.

The *probability density function* $f(x)$ is defined by the limit of

$$f(x)\Delta x = P\{x \le x' \le x + \Delta x\}, \tag{7-2}$$

as $\Delta x \to 0$. Thus $f(x)\Delta x$ is just the probability that x' will take on a value between x and $x + \Delta x$. Clearly we must have $f(x) \ge 0$, and

$$\int_a^b f(x)\,dx = P\{a \le x \le b\}. \tag{7-3}$$

If x may take on any real value between $-\infty$ and $+\infty$, we require that the probability density function be normalized by

$$\int_{-\infty}^{\infty} f(x)\,dx = 1. \tag{7-4}$$

On the other hand, if the values of x are restricted to between x^- and x^+, then we require normalization over the restricted domain

$$\int_{x^-}^{x^+} f(x)\,dx = 1. \tag{7-5}$$

The *cumulative probability distribution function*, defined by

$$F(x) = P\{x' \leq x\}, \tag{7-6}$$

is the probability that the random variable x' is less than or equal to x. From our definition of $f(x)$ we have for a random variable that can take on only real values,

$$F(x) = \int_{-\infty}^{x} f(x')\,dx'. \tag{7-7}$$

From this we see that

$$\lim_{x \to \infty} F(x) \equiv F(\infty) = 1, \tag{7-8}$$

$$\lim_{x \to -\infty} F(x) \equiv F(-\infty) = 0, \tag{7-9}$$

and using Eqs. 7-3 and 7-7, we have

$$P\{a \leq x' \leq b\} = F(b) - F(a). \tag{7-10}$$

Finally, it is often more convenient to write Eq. 7-7 in the differential form

$$\frac{dF(x)}{dx} = f(x). \tag{7-11}$$

The relationship between $f(x)$ and $F(x)$ is shown in Fig. 7-1.

To make use of $f(x)$ or $F(x)$ in Monte Carlo calculations we first must introduce the rules for transformation of random variables. Suppose

$$y = y(x) \tag{7-12}$$

is a function of the random variable x. If $g(y)\,dy$ is the probability that y is between y and $y + dy$, and $f(x)\,dx$ is the probability that x is between x and $x + dx$, the probability density functions $g(y)$ and $f(x)$ must satisfy

$$|g(y)\,dy| = |f(x)\,dx|, \tag{7-13}$$

or since $g(y) > 0$ and $f(x) > 0$,

$$g(y) = f(x)\left|\frac{dx}{dy}\right|. \tag{7-14}$$

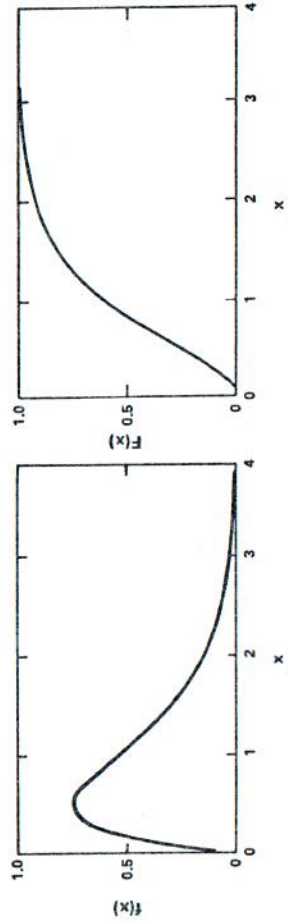

Figure 7-1 Example of (*a*) probability density function and (*b*) the resulting cumulative probability distribution function.

In Chapter 1 we encountered such transformations, for example, in converting from speed ($x = v$) to energy ($y = E$) distributions of neutrons.

Now suppose we consider one very particular function, $y = F(x)$ of the random variable x, where $F(x)$ is the cumulative probability distribution. Then Eq. 7-14 becomes

$$g(F) = f(x)\left|\frac{dx}{dF}\right|. \tag{7-15}$$

If we now use Eq. 7-11 to evaluate the derivative on the right, we obtain for this particular transformation simply

$$g(F) = 1, \qquad 0 \le F \le 1. \tag{7-16}$$

Since $g(F)$ is just the probability density function of the random variable F, this equation just states that the probability of F taking on a value between F and $F + dF$ is just equal to dF. Thus F is uniformly distributed between zero and one.

We may now show the relevance of these relationships to Monte Carlo calculations. Random number generators—or more correctly pseudo random number generators—available on digital computers provide sequences of numbers, ξ, that are uniformly distributed between zero and one.[5,11] We may therefore use such a generator to sample uniformly distributed $F(x)$ in an unbiased manner:

$$F(x) = \xi. \tag{7-17}$$

Thus by repeatedly calling the random number generator for values of ξ we obtain an unbiased distribution of $F(x)$ values. It is the distribution of x and not of $F(x)$, however, that we need to sample. Therefore, after each call to the random number generator we must perform the inversion

$$x = F(\xi)^{-1}. \tag{7-18}$$

Indeed the inversion of the cumulative probability distributions representing physical processes is central to accurate and economical Monte Carlo simulation of particle transport. A number of techniques may be used to perform this inversion. In what follows, we carry out some examples that are relevant to particle transport problems.

Distribution Sampling

First, suppose we want to generate a series of random numbers that are distributed according to the number of mean free paths that particles will travel between collisions. From Eqs. 1-5 through 1-7 we know that if $0 < x < \infty$ is the distance in mean free paths, then the probability density function is

$$f(x) = e^{-x}, \tag{7-19}$$

and the cumulative probability distribution is

$$F(x) = 1 - e^{-x}. \tag{7-20}$$

Physically, $f(x)\,dx$ is the probability that a particle starting at $x = 0$ will make a collision between x and $x + dx$, while $F(x)$ is the probability that it will make a collision within the distance x. For this simple relationship we may perform the inversion of Eq. 7-18 directly to obtain

$$x = -\ln(1 - \xi). \tag{7-21}$$

Moreover, if ξ is uniformly distributed between 0 and 1 so will be $1 - \xi$, so that we simply write

$$x = -\ln \xi. \tag{7-22}$$

Aside from this straightforward evaluation of probability distributions by inversion there are alternative methods that may prove to be beneficial, particularly if the inverse of $F(x)$ is costly to obtain or if $f(x)$ is given as numerical data. We illustrate two of these methods: the rejection technique and numerical evaluation. Suppose that $f(x)\,dx$ is the fraction of source particles born between x and $x + dx$. If $F(\xi)^{-1}$ is costly to evaluate we may consider the rejection technique in which such evaluation is replaced by the generation of additional random numbers.

Suppose that $0 \le x \le a$ and $0 \le f(x) \le f_{\max}$. We then define $x' = x/a$ and $\tilde{f}(x') = f(ax')/f_{\max}$. A graph of $\tilde{f}(x')$ would then fit in a unit square as shown in Fig. 7-2. To obtain the distribution of x' and therefore of x we choose pairs of random numbers ξ_1 ad ξ_2 uniformly distributed between zero and one. We let $x' = \xi_1$, and then ask, "Is $\xi_2 \le \tilde{f}(\xi_1)$?" If it is, we use $x' = \xi_1$. If $\xi_2 > \tilde{f}(\xi_1)$, we reject x' and choose another pair of random numbers. In this way the number of random numbers chosen and not rejected between x' and $x' + \Delta x'$ is just proportional to $\tilde{f}(x')\Delta x'$ as required. Note that we need not evaluate $F(\xi)^{-1}$. On the other hand, if the area under the curve

$$\int_0^1 dx' \tilde{f}(x') \tag{7-23}$$

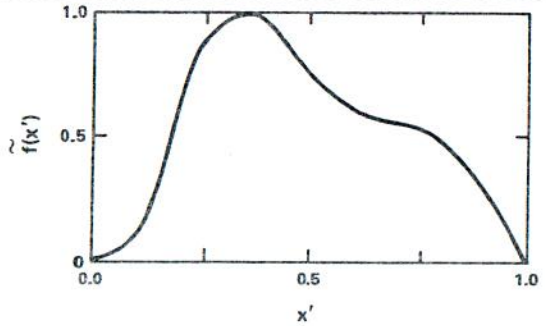

Figure 7-2 Scaled probability density function.

is small compared to unity, most of the random number pairs will be rejected and this procedure will become quite inefficient.

A third procedure may be used in the event that the function is given as numerical data from a histogram, as shown in Fig. 7-3*a*. The corresponding $F(x)$ will be a continuous piecewise linearly increasing function as shown in Fig. 7-3*b*. Thus $F(x)$ may be shown to have the form

$$F(x) = \frac{1}{x_i - x_{i-1}}\left[(x - x_{i-1})F_i + (x_i - x)F_{i-1}\right] \qquad x_{i-1} < x \le x_i \tag{7-24}$$

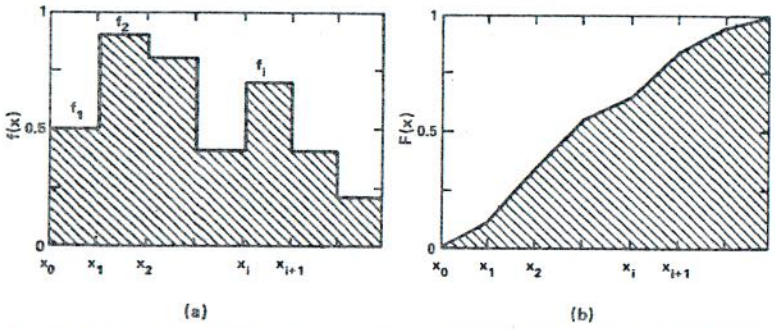

Figure 7-3 The (*a*) probability density function and (*b*) cumulative probability distribution functions constructed from discrete data.

where

$$F_i = \sum_{i'=1}^{i} f_{i'}(x_{i'} - x_{i'-1}). \tag{7-25}$$

Hence to obtain $x = F^{-1}(\xi)$ indirectly we first pick a uniformly distributed random number ξ. We search to determine which interval ξ is in. After finding the interval $F_{i-1} < \xi < F_i$ we set $F(x) = \xi$ in Eq. 7-24 and solve for x:

$$x = \frac{(x_i - x_{i-1})\xi - x_i F_{i-1} + x_{i-1}F_i}{F_i - F_{i-1}}. \tag{7-26}$$

Thus far we have considered only continuous sampling procedures. We also have need for discrete sampling, where we need to know not the values of x but only the answer to a question such as "Does a collision take place in a certain region?" or "Does a collision result in fission, capture, elastic scattering, or inelastic scattering?" To obtain our answer with a random number generator we simply note that

$$\sigma = \sigma_f + \sigma_\gamma + \sigma_n + \sigma_{n'} \tag{7-27}$$

and divide the unit line into intervals of length σ_f/σ, σ_γ/σ, σ_n/σ, $\sigma_{n'}/\sigma$ as shown in Fig. 7-4. We then simply choose a random number ξ uniformly distributed between zero and one and determine into which of these intervals it falls.

Functions of Two Random Variables

Probability distributions may also be defined as a function of more than one random variable.[4,12] For example, if we have two random variables x and y

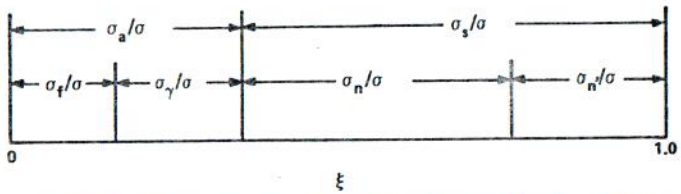

Figure 7-4 A unit line representation of the conditional probabilities for various types of neutron interactions.

then we may define a joint probability density function

$$P\{x \le x' \le x + \Delta x, y \le y' \le y + \Delta y\} = f(x, y)\,\Delta x\,\Delta y. \quad (7\text{-}28)$$

The normalization for the joint probability density function is

$$\int_{-\infty}^{\infty} dx \int_{-\infty}^{\infty} dy f(x, y) = 1 \quad (7\text{-}29)$$

since both x and y must lie between $-\infty$ and $+\infty$. If we integrate over only one of the variables, we obtain

$$g(x) = \int_{-\infty}^{\infty} dy f(x, y), \quad (7\text{-}30)$$

$$h(y) = \int_{-\infty}^{\infty} dx f(x, y). \quad (7\text{-}31)$$

These qualities are referred to as the marginal probability densities of x and y respectively. Also associated with the joint probability density function $f(x, y)$ is a joint cumulative probability distribution

$$P\{x' \le x, y' \le y\} = F(x, y) \quad (7\text{-}32)$$

which may be written as

$$F(x, y) = \int_{-\infty}^{x} dx' \int_{-\infty}^{y} dy' f(x', y'). \quad (7\text{-}33)$$

In Monte Carlo calculations these bivariate distributions normally take one of two limiting forms either with x and y independent of one another or with x conditional on the value of y. If the joint probability density function is separable in the form

$$f(x, y) = f_1(x) f_2(y), \quad (7\text{-}34)$$

then x and y are said to be independent.

An example of independence occurs in choosing the direction of particles produced or scattered isotropically in the laboratory system. The production is proportional to the solid angle $d\Omega$:

$$f(\hat{\Omega})\,d\Omega = C\,d\Omega \quad (7\text{-}35)$$

where C is a constant. Since $\int d\Omega = 1$, we must have $C = f(\hat{\Omega}) = 1$. Now,

$d\Omega$ may be written in terms of (θ, ω), the polar and azimuthal coordinates

$$d\Omega = \frac{d\theta \sin\theta\, d\omega}{4\pi} = \left(\frac{d\mu}{2}\right)\left(\frac{d\omega}{2\pi}\right), \quad (7\text{-}36)$$

where $\mu = \cos\theta$. Note that normalization of Eq. 7-35 requires that $f(\mu, \omega) = 1/(4\pi)$. Clearly Eq. 7-36 is in the form of Eq. 7-34,

$$f(\mu, \omega) = f_1(\mu) f_2(\omega), \quad (7\text{-}37)$$

where $f_1(\mu) = \frac{1}{2}$ and $f_2(\omega) = 1/(2\pi)$. Hence μ and ω are to be sampled independently. We may use Eq. 7-18 with analytical inversion to determine the particle direction from

$$\mu = 2\xi_1 - 1, \qquad \omega = 2\pi\xi_2, \quad (7\text{-}38)$$

where ξ_1 and ξ_2, are uniformly distributed independent random numbers.

Two random variables x and y may also be related by a conditional probability distribution. Thus

$$P\{x \le x' \le x + \Delta x | y\} \equiv f(x|y)\,\Delta x \quad (7\text{-}39)$$

is just the probability that x will lie between x and $x + \Delta x$ given the condition that a particular value y is taken by the second random variable. The conditional probability density function of x, given y, is defined in terms of joint and marginal distributions,

$$f(x|y) = \frac{f(x, y)}{h(y)}, \qquad h(y) \ne 0, \quad (7\text{-}40)$$

where $h(y)$ is defined by Eq. 7-31.

As an application of conditional probabilities that we use in Section 7-5, consider neutrons emitted as shown in Fig. 7-5 at a distance y from the outer surface of a solid, V. The solid is assumed to be a purely absorbing material. We may calculate the conditional probability $f(x|y)$ that a neutron emitted as shown will travel a distance between x and dx in the solid, given that the distance to the surface is y. Since the neutron history may be terminated by either of two mechanisms—collision or escape—the probability density function will have two contributions.

For $x < y$ the probability that a neutron will travel a distance between x and $x + dx$ is the same as in Eq. 7-19; for example, the probability density that the neutron will collide between x and $x + dx$ is

$$f(x|y) = \sigma e^{-\sigma x}, \qquad x < y. \quad (7\text{-}41)$$

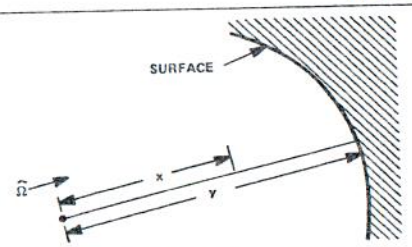

Figure 7-5 Streaming path for neutrons emitted a distance y from the surface of a solid.

The probability that the neutron will collide before escaping is just

$$\int_0^y dx f(x|y) = 1 - e^{-\sigma y}. \tag{7-42}$$

And hence the escape probability is

$$1 - \int_0^y dx f(x|y) = e^{-\sigma y}. \tag{7-43}$$

Hence there is a probability $e^{-\sigma y}$ that a neutron will travel exactly a distance y in the solid. This discrete probability may be combined with Eq. 7-41 through the use of a Dirac delta and Heavyside functions to obtain the conditional probability density function traveling a distance in the solid x, given a boundary at distance y:

$$f(x|y) = \sigma e^{-\sigma x} H(y - x) + e^{-\sigma y}\delta(x - y), \qquad x \geq 0, \tag{7-44}$$

where

$$H(x) = \begin{cases} 0, & x < 0 \\ 1, & x \geq 0 \end{cases} \tag{7-45}$$

is the Heavyside function, and, of course, $f(x|y) = 0$ for $x < 0$.

The marginal density function $h(y)$ of the path lengths to the surface will depend on the space-angle distribution in which neutrons are emitted as well as on the size and shape of the solid. For any path length distribution $h(y)$ we may write Eq. 7-44 as

$$f(x, y) = h(y) f(x|y), \tag{7-46}$$

and it is easily shown that Eq. 7-40 holds for $f(x, y)$.

7-3 ANALOG MONTE CARLO SAMPLING

With the information we have gained regarding distributions of random variables we are now prepared to construct a simple analog Monte Carlo game. For the present we restrict ourselves to monoenergetic transport in a solid with isotropic scattering and space-independent cross sections. While the general treatment of energy and of complex multiregion systems gives Monte Carlo much of its power, for now some of the statistical considerations can be made more transparent using this simplified problem. The energy variable will be added in a straightforward way, and the geometrical tracking of particles through complex configurations is taken up in Section 7-7.

Tracking Procedure

Suppose the source distribution is $S(x, y, z)$. Then by generating three random numbers, the technique of the preceding section can be used to set the starting point in space of the history. Two more random numbers used in conjunction with Eq. 7-36 then determine the particle direction. Equation 7-22 may then be used to determine the number of mean free paths traveled before the next collision. With this information and the cross section, the x, y, z position of the first collision is determined. If the particle passes out of V, the problem domain, in less than the calculated number of mean free paths, it has escaped, and the history is terminated. If it collides within V, then a random number is generated, and if $\xi < \sigma_a/\sigma$, the particle is absorbed and the history is terminated. If $\xi \geq \sigma_s/\sigma$, the particle is scattered. The foregoing procedure is repeated for each independent history, starting again with the generation of two random numbers to determine the particle's direction after collision. This cycle of determining the direction, distance traveled, next collision point, and type of collision is repeated until the particle either escapes from the system or is absorbed. The geometry of the solid enters the calculation in determining whether a boundary is closer than the distance to collision, that is, whether a collision occurs within the solid.

The analog Monte Carlo simulation consists of repeating the foregoing procedure for N independent histories. As referred to earlier, the result of the calculation usually consists of a *sample mean*,

$$\hat{x} = \frac{1}{N} \sum_{n=1}^{N} x_n, \tag{7-47}$$

where x is some property of the histories.

Tallies

Since the histories are random, x also is a random variable. It does not in general coincide with the random variables that are sampled in producing the histories: the scattering angles, positions, and distances between collisions. Rather, x most often is related to scalar flux, current distribution, escape probability, or one of the other dependent variables that are sought from the solution of the transport equation. Our task then is to ask which of the properties that we have available from the simulation of random particle histories should be tallied in order to calculate the scalar flux, current, or other parameters of interest.

For scalar flux the two most widely used tallies result from the relationship between collision density and scalar flux and from the definition of scalar flux in terms of total neutron track length, both discussed in Chapter 1. Suppose that we want to calculate the average scalar flux $\bar{\phi}$ in some volume $\tilde{V}$ where the total cross section is $\bar{\sigma}$. Then since $\bar{\sigma}\bar{\phi}$ is the collision density; $\bar{c}$, the mean number of collisions in V per unit time, is

$$\bar{c} = \tilde{V}\bar{\sigma}\bar{\phi}. \tag{7-48}$$

Hence for the Monte Carlo simulation we may write

$$\bar{\phi} = \frac{1}{\tilde{V}\bar{\sigma}}\bar{c}, \tag{7-49}$$

where $\bar{c}$ is the mean number of collisions, normalized to one source particle. The random variable whose mean we want to calculate is thus $\bar{c}$, the mean number of collisions per neutron history in $\tilde{V}$. If we normalize our calculation to a source strength of one neutron, we then have a sample estimate of $\hat{c}$:

$$\hat{c} = \frac{1}{N}\sum_n c_n, \tag{7-50}$$

where c_n is the number of collisions made in $\tilde{V}$ during the nth history. Our sample estimate of the scalar flux is then

$$\hat{\phi} = \frac{1}{\tilde{V}\bar{\sigma}}\frac{1}{N}\sum_n c_n. \tag{7-51}$$

A shortcoming of this estimate of the scalar flux lies in the fact that only particles that collide in $\tilde{V}$ will contribute to the collision estimator $\hat{\phi}$. We

next discuss the path length estimator for which every particle that passes through $\tilde{V}$ contributes, whether or not a collision occurs. Recall from Chapter 1 that the scalar flux may be defined as the total track length traversed by all particles per unit volume per unit time. Hence

$$\bar{\phi} = \frac{1}{\tilde{V}}\bar{l}, \tag{7-52}$$

where $\bar{l}$ is the mean track length normalized to one source particle. If we have a Monte Carlo simulation of N particles, we therefore estimate the mean value $\bar{l}$ of the random variable l by

$$\hat{l} = \frac{1}{N}\sum_n l_n, \tag{7-53}$$

where l_n is the track length in $\tilde{V}$ of the nth particle. Note that l_n may consist of more than one contribution since a single particle may pass through the volume $\tilde{V}$ more than once. From Eqs. 7-52 and 7-53 we then have as our path length flux estimator

$$\hat{\phi} = \frac{1}{\tilde{V}}\frac{1}{N}\sum_n l_n. \tag{7-54}$$

We would also like to be able to estimate particle currents, for if currents can be determined, escape probabilities and other particle balance properties follow immediately. Suppose we want to calculate the mean value of the current crossing surface $\tilde{A}$ in the $\hat{n}$ direction,

$$\tilde{A}\bar{J} = \tilde{A}\left(\bar{J}_+ - \bar{J}_-\right), \tag{7-55}$$

where $\bar{J}_+$ and $\bar{J}_-$ are the mean values of the partial currents in the positive and negative directions. We may write

$$\tilde{A}\bar{J}_+ = \bar{p}^+ \quad \text{and} \quad \tilde{A}\cdot\bar{J} = \bar{p}^-, \tag{7-56}$$

where $\bar{p}^{\pm}$ are the mean numbers of particles passing through the surface per second in the positive and negative directions respectively. These quantities can be estimated from our Monte Carlo sample as

$$\hat{p}^{\pm} = \frac{1}{N}\sum_n p_n^{\pm} \tag{7-57}$$

where p_n^+ and p_n^- are the number of passages through the surface $\tilde{A}$ made

by the nth particle history in the positive and negative direction respectively. We have

$$\hat{J}_+ = \frac{1}{\bar{A}}\frac{1}{N}\sum_n p_n^+, \qquad \hat{J}_- = \frac{1}{\bar{A}}\frac{1}{N}\sum_n p_n^-, \tag{7-58}$$

and

$$\hat{J} = \hat{J}_+ - \hat{J}_- \tag{7-59}$$

is an approximation to the net current.

It is also possible to calculate the average scalar flux over a surface by using the relationship among angular flux, scalar flux, and current, which is given in Chapter 1. It may be shown that the value of $\bar{\phi}$ on $\bar{A}$ may be estimated from

$$\hat{\phi} = \frac{1}{\bar{A}}\frac{1}{N}\sum_n \zeta_n \tag{7-60}$$

where ζ_n is the number of crossings of the nth neutron, each weighted by $|1/\mu|$, where $\mu = \hat{\Omega} \cdot \hat{n}$ is the direction cosine of the particle with respect to the positive normal to the surface. Thus if there were I crossings in the nth history,

$$\zeta_n = \sum_{i=1}^{I} \left|\frac{1}{\mu_i}\right|. \tag{7-61}$$

A difficulty arises if one must calculate the flux over a very small volume or surface, as is the case, for example, when it is desired to determine the response of a "point" detector in a system. The foregoing tallies become useless, since if the volume is very small no histories are likely to collide in it, or even to pass through it. In such circumstances there are two alternatives. One may use an adjoint Monte Carlo calculation in which particles are emitted from the detector volume,[2,13] or one may resort to one of the more subtle tallying techniques for the estimate of the flux at a point.[7,14-16] We defer discussion of the use of the adjoint equation until Section 7-6; estimates of the flux at a point and some of the tallies are treated in Section 7-7.

Before proceeding, it is important to note that it is common practice to normalize Monte Carlo results to a source of one particle, while in steady-state deterministic transport calculations the source is normally given in terms of particles per second. Thus the foregoing tallies have units of cm^{-2} rather than particles/cm^2/sec as in deterministic calculations. For steady-state calculations, however, the correspondence is clear. The results of the Monte Carlo calculation are just multiplied by the number of particles produced per second; the magnitudes of the tallies are then correct, and the units become particles/cm^2/sec.

7-4 ERROR ESTIMATES

In the preceding section we indicated how to use a number of random variables to estimate the scalar flux and current in analog Monte Carlo calculations. The question now arises as to how much error the sample estimate $\hat{\phi}$ or $\hat{J}$ is likely to have in relation to the true values of the mean $\bar{\phi}$ or $\bar{J}$. To make an estimation of the statistical uncertainty of our results, we must go back to the properties of a random variable, introduce the concepts of expectation values and variance, and utilize the central limit theorem to arrive at an error estimate.

In the following discussion we designate the random variables c, l, p^+, p^-, ζ used in the preceding section to estimate flux or current as x. For a particular simulation in principle there exists a probability density function $f(x)$ for each of these estimators. Of course we can never determine this function exactly unless the problem is so simple that it can be solved analytically; otherwise an infinite number of particle histories would be required. Estimating the properties of $f(x)$, however, leads in turn to an estimate of the error in $\hat{x}$.

The functional dependence of $f(x)$ on x may have different forms depending on which of the estimators is under consideration. For example, the collision and surface crossing estimators c_n and p_n^+ and p_n^- can take on only integer values. Hence the probability density function has the form

$$f(x) = \sum_i p_i \delta(x - i), \tag{7-62}$$

where

$$\sum_i p_i = 1, \tag{7-63}$$

while the coefficients p_i determine the distribution. A special case of Eq. 7-62 is the binomial estimator

$$f(x) = p_0\delta(x) + [1 - p_0]\delta(x - 1), \tag{7-64}$$

where the estimator can take on only values of zero and one. This would be

the case, for example, with the collision estimator c in a pure absorber problem, for then each history would result in either zero or one collision.

The path length estimator l and the surface flux estimator ζ result in continuous $f(x)$ distributions with $0 \le x \le \infty$ for l and $0 \le |x| \le \infty$ for ζ. In many Monte Carlo problems mixed probability distributions also occur. If some of the neutrons do not contribute to a particular quantity, there will be a delta function at $x = 0$, but at the same time those neutrons that do contribute may result in a continuous distribution, as is the case with the path length estimator. Such distributions are discussed in detail in Section 7-6.

Expectation Values

Suppose that x is a random variable, for example, some property of a Monte Carlo history. The expectation value of x is defined as

$$E[x] \equiv \int_{-\infty}^{\infty} xf(x)\,dx \tag{7-65}$$

where $f(x)$ is the probability density distribution. Qualitatively, it is the mean value of x that we would expect to achieve if we repeated a Monte Carlo calculation infinitely many times. Moreover, if we drew random and independent samples, $x_1, x_2, \ldots, x_n$, from $f(x)$, the expectation value of any one x_n would be

$$E[x_n] = E[x]. \tag{7-66}$$

This expression states that the average value of x_n is equal to the expectation or *true mean* value

$$\bar{x} = \int_{-\infty}^{\infty} xf(x)\,dx. \tag{7-67}$$

Thus the expectation value of $\hat{x}$ in Eq. 7-1 may also be shown to be equal to $\bar{x}$:

$$E[\hat{x}] = E\left[\frac{1}{N}\sum_{n=1}^{N} x_n\right] = \frac{1}{N}\sum_{n=1}^{N} E[x_n] = E[x] = \bar{x}. \tag{7-68}$$

Thus $\hat{x}$ is said to be an unbiased estimator of $\bar{x}$.

The foregoing results do not imply, however, that x_n or even $\hat{x}$ will be equal to $\bar{x}$. What is needed is a measure of the spread in values of $\hat{x}$ about $\bar{x}$. To do this we must first introduce some functions of a random variable.[4]

Suppose that $g(x)$ is a real function of the random variable x. The expectation value of $g(x)$ is then defined by

$$E[g(x)] \equiv \bar{g} = \int_{-\infty}^{\infty} g(x)f(x)\,dx. \tag{7-69}$$

Corresponding to Eq. 7-66 if we draw $x_1, x_2, \ldots, x_n$ independently from $f(x)$, then

$$E[g(x_n)] = E[g(x)]. \tag{7-70}$$

Moreover, we note that if g is a linear combination

$$g(x) = C_1 g_1(x) + C_2 g_2(x), \tag{7-71}$$

where C_1 and C_2 are constants, then

$$E[g(x)] = C_1 E[g_1(x)] + C_2 E[g_2(x)]. \tag{7-72}$$

These definitions may be generalized to more than one random variable. For example, if $f(x, y)$ is the joint probability density function for x and y, the expectation value of a function $g(x, y)$ will be

$$E[g(x, y)] = \int_{-\infty}^{\infty} dx \int_{-\infty}^{\infty} dy\, g(x, y)f(x, y). \tag{7-73}$$

Moreover, choosing random variables x_n and $y_{n'}$ from $f(x, y)$ we have

$$F[g(x_n, y_{n'})] = E[g(x, y)]. \tag{7-74}$$

Variance

To estimate the spread of values of x, and eventually of $\hat{x}$, about $\bar{x}$ we introduce a particular function; the second moment about the mean

$$g(x) \equiv (x - \bar{x})^2. \tag{7-75}$$

Then by using Eq. 7-69, the *variance* is defined to be

$$\sigma^2(x) \equiv E\left[(x - \bar{x})^2\right] = \int_{-\infty}^{\infty} dx(x - \bar{x})^2 f(x). \tag{7-76}$$

This expression may be simplified by substituting

$$(x - \bar{x})^2 = x^2 - 2x\bar{x} + \bar{x}^2 \tag{7-77}$$

into the definition to obtain

$$\sigma^2(x) = \int_{-\infty}^{\infty} dx\, x^2 f(x) - 2\bar{x}\int_{-\infty}^{\infty} dx\, x f(x) + \bar{x}^2 \int_{-\infty}^{\infty} dx\, f(x) \quad (7\text{-}78)$$

or simply

$$\sigma^2(x) = \overline{x^2} - \bar{x}^2, \quad (7\text{-}79)$$

where

$$\overline{x^n} \equiv \int_{-\infty}^{\infty} dx\, x^n f(x). \quad (7\text{-}80)$$

The variance, or more particularly the *standard deviation*,

$$\sigma(x) = \left(\overline{x^2} - \bar{x}^2\right)^{1/2}, \quad (7\text{-}81)$$

provides a measure of the spread of x about the mean value $\bar{x}$.

We may now express the variance of $\hat{x}$ in terms of the variance of x. We define

$$\sigma^2(\hat{x}) = E\left[(\hat{x} - \bar{x})^2\right]. \quad (7\text{-}82)$$

Hence

$$\sigma^2(\hat{x}) = E\left[\left(\frac{1}{N}\sum_{n=1}^{n} x_n - \bar{x}\right)^2\right]$$

$$= E\left[\left\{\frac{1}{N}\sum_{n=1}^{N}(x_n - \bar{x})\right\}^2\right]. \quad (7\text{-}83)$$

Since we may expand the square of the sum as

$$\left\{\sum_n (x_n - \bar{x})\right\}^2 = \sum_n (x_n - \bar{x})^2 + \sum_{n \neq n'}\sum (x_n - \bar{x})(x_{n'} - \bar{x}), \quad (7\text{-}84)$$

Eq. 7-83 becomes

$$\sigma^2(\hat{x}) = \frac{1}{N^2}\sum_{n=1}^{N} E\left[(x_n - \bar{x})^2\right] + \frac{1}{N^2}\sum_{n \neq n'}\sum E\left[(x_n - \bar{x})(x_{n'} - \bar{x})\right], \quad (7\text{-}85)$$

where we have used the fact that the expectation value of the sum is equal to the sum of the expectation values.[12] Expanding the first term yields

$$\left[E(x_n - \bar{x})^2\right] = E\left[x_n^2\right] - 2\bar{x}E\left[x_n\right] + \bar{x}^2. \quad (7\text{-}86)$$

Then utilizing Eq. 7-66 we have

$$E\left[(x_n - \bar{x})^2\right] = \overline{x^2} - \bar{x}^2 = \sigma^2(x). \quad (7\text{-}87)$$

If x_n and $x_{n'}$, $n \neq n'$, are drawn independently from $f(x)$, then the second term may be shown to vanish:

$$E\left[(x_n - \bar{x})(x_{n'} - \bar{x})\right] = E\left[x_n x_{n'}\right] - \bar{x}E\left[x_n\right] - \bar{x}E\left[x_{n'}\right] + \bar{x}^2; \quad (7\text{-}88)$$

but since $E[x_n] = E[x_{n'}] = \bar{x}$, we have

$$E\left[(x_n - \bar{x})(x_{n'} - \bar{x})\right] = E\left[x_n x_{n'}\right] - \bar{x}^2. \quad (7\text{-}89)$$

If x_n and $x_{n'}$ are both independent samplings of $f(x)$, however, the definition of independence in Eq. 7-34 leads us to

$$f(x, x') = f(x)f(x') \quad (7\text{-}90)$$

and thus

$$E\left[x_n x_{n'}\right] = \left[\int_{-\infty}^{\infty} x f(x)\, dx\right]^2 = \bar{x}^2, \quad (7\text{-}91)$$

causing $E[(x_n - \bar{x})(x_n' - \bar{x})]$ to vanish. Thus combining Eqs. 7-85 and 7-87, we obtain the desired result:

$$\sigma^2(\hat{x}) = \frac{1}{N}\sigma^2(x). \quad (7\text{-}92)$$

Thus the standard deviation is given by

$$\sigma(\hat{x}) = \frac{\sigma(x)}{\sqrt{N}}. \quad (7\text{-}93)$$

This result may be interpreted as follows: $\sigma(x)$ is a measure of the spread of individual x_n drawn from a probability density distribution $f(x)$ about

$\bar{x}$. If we use $\hat{x}$ constructed from N values of x_n according to Eq. 7-1 to estimate $\bar{x}$, then the spread in our results—if we repeated the calculation for $\hat{x}$ many times—of $\hat{x}$ about $\bar{x}$ is proportional to $\sigma(x)$ and falls off as the square root of the number of histories in the sample.

In order to estimate the spread in $\hat{x}$ we must also be able to make an unbiased estimate $\sigma^2(x)$ from a finite number of histories, an unbiased estimator being one with the correct expectation value. In this case the *sample variance* defined by

$$S^2 = \frac{1}{N-1}\sum_{n=1}^{N}(x_n - \hat{x})^2 \tag{7-94}$$

can be shown to meet the condition $E[S^2] = \sigma^2(x)$ as follows. First

$$E[S^2] = \frac{1}{N-1}E\left[\sum_{n=1}^{N}(x_n - \hat{x})^2\right]. \tag{7-95}$$

By writing $x_n - \hat{x} = (x_n - \bar{x}) - (\hat{x} - \bar{x})$ and using the definition of $\hat{x}$, it may be shown that

$$\sum_{n=1}^{N}(x_n - \hat{x})^2 = \sum_{n=1}^{N}(x_n - \bar{x})^2 - N(\hat{x} - \bar{x})^2. \tag{7-96}$$

Thus

$$E[S^2] = \frac{1}{N-1}\left\{\sum_{n=1}^{N}E\left[(x_n - \bar{x})^2\right] - NE\left[(\hat{x} - \bar{x})^2\right]\right\}. \tag{7-97}$$

From Eq. 7-87, $E[(x_n - \bar{x})^2] = \sigma^2(x)$, while from Eqs. 7-82 and 7-92

$$E\left[(\hat{x} - \bar{x})^2\right] = \frac{\sigma^2(x)}{N}. \tag{7-98}$$

Thus

$$E[S^2] = \frac{1}{N-1}\left\{N\sigma^2(x) - \frac{N\sigma^2(x)}{N}\right\} = \sigma^2(x). \tag{7-99}$$

Thus we have shown that the sample variance is an unbiased estimator of $\sigma^2(x)$. In practice it is not calculated directly from Eq. 7-94 but rather the square term is multiplied out so that

$$S^2 = \frac{N}{N-1}(\widehat{x^2} - \hat{x}^2) \tag{7-100}$$

where

$$\widehat{x^2} \equiv \frac{1}{N}\sum_{n=1}^{N}x_n^2. \tag{7-101}$$

From this the *sample standard deviation*

$$S = \left(\frac{N}{N-1}\right)^{1/2}\left\{\frac{1}{N}\sum_{n=1}^{N}x_n^2 - \hat{x}^2\right\}^{1/2} \tag{7-102}$$

is calculated. Moreover, when large numbers of histories are involved, $N/(N-1)$ often is set equal to one.

The Central Limit Theorem

With the establishment of algorithms for making unbiased estimates of the mean and variance, we are now in a position to utilize one of the strongest results of probability theory; the central limit theorem.[4, 12] Suppose that Monte Carlo calculations are carried out, each consisting of independent histories, such that the x_n are drawn from the same distribution having a finite mean and variance. For any fixed value of N histories per calculation, there is a probability density function, say $f_N(\hat{x})$, which describes the distribution of the $\hat{x}$ that results from repeated Monte Carlo calculations. As N approaches infinity, the central limit theorem states that there is a specific limiting distribution for the resulting values of $\hat{x}$, and this is the normal distribution:

$$f_N(\hat{x}) \approx \frac{1}{\sqrt{2\pi}\,\sigma(\hat{x})}\exp\left[\frac{-(\hat{x} - \bar{x})^2}{2\sigma^2(\hat{x})}\right], \qquad N \to \infty. \tag{7-103}$$

Moreover, since we already related $\sigma^2(\hat{x})$ to $\sigma^2(x)$ by Eq. 7-92 we may write

$$f_N(\hat{x}) = \sqrt{\frac{N}{2\pi}}\,\frac{1}{\sigma(x)}\exp\left[\frac{-N(\hat{x} - \bar{x})^2}{2\sigma^2(x)}\right], \qquad N \to \infty. \tag{7-104}$$

Provided N is sufficiently large, we may now use the form of $f(\hat{x})$ to eliminate the error in $\hat{x}$ given N, the number of particles per batch, and $\sigma^2(x)$ the variance of our random variable distribution. While in practice we cannot calculate $\sigma^2(x)$ exactly, we can estimate it from the sample variance $S^2(x)$ given by Eq. 7-94.

Suppose we want to know the probability that $\hat{x}$ is between $\bar{x} - \varepsilon$ and $\bar{x} + \varepsilon$. From Eq. 7-3 we may write

$$P\{\bar{x} - \varepsilon < \hat{x} < \bar{x} + \varepsilon\} = \int_{\bar{x}-\varepsilon}^{\bar{x}+\varepsilon} f_N(\hat{x})\, d\hat{x}. \tag{7-105}$$

Inserting Eq. 7-104 and changing variables with $\sqrt{2/N}\, t = (\hat{x} - \bar{x})/\sigma(x)$, we have

$$p\{\bar{x} - \varepsilon < \hat{x} \le \bar{x} + \varepsilon\} = \frac{2}{\sqrt{\pi}} \int_0^{(\sqrt{N/2})(\varepsilon/\sigma)} dt\, e^{-t^2}, \tag{7-106}$$

or using the definition of the error function

$$P\{\bar{x} - \varepsilon \le \hat{x} \le \bar{x} + \varepsilon\} = \operatorname{erf}\left[\sqrt{\frac{N}{2}}\, \frac{\varepsilon}{\sigma(x)}\right]. \tag{7-107}$$

Thus given an ε we need only to evaluate the standard error integral to determine the probability that $\hat{x}$ will fall into the interval $\bar{x} \pm \varepsilon$. If we take $\varepsilon = .674\sigma(x)/\sqrt{N}$ we have a 50% probability that the value of x will fall into the interval $x \pm .6740\sigma(x)/\sqrt{N}$. More frequently when plus or minus errors are tabulated for Monte Carlo calculations, they correspond to $\varepsilon = \sigma(x)/\sqrt{N}$ (i.e., that $\hat{x}$ is within one standard deviation of $\bar{x}$, the true mean). Hence evaluating erf$[1/\sqrt{2}]$ we find that these values correspond to a probability of 68.3% that the sample mean $\hat{x}$ will lie within the interval $\bar{x} - \sigma(x)/\sqrt{N}$ to $\bar{x} + \sigma(x)/\sqrt{N}$. Two or three standard deviations may also be used if higher confidence levels are desired. For example,

$$P\left\{\bar{x} - \frac{M\sigma(x)}{\sqrt{N}} \le \hat{x} \le \bar{x} + \frac{M\sigma(x)}{\sqrt{N}}\right\} = \begin{cases} .6826, & M = 1, \\ .954, & M = 2, \\ .997, & M = 3. \end{cases} \tag{7-108}$$

In using the foregoing error estimates some cautionary notes are warranted. No matter what quantity is being estimated, the value of N must be large for the foregoing expressions to hold, not only because the central limit theorem applies only for large N, but also because a large number of histories is required for Eq. 7-102 to give a reliable estimate of $\sigma(x)$. One of the most subtle problems in Monte Carlo calculations lies in determining how many histories are required for a particular problem before these estimates have validity. It can be very dangerous, for example, to simply run N histories and take the error estimate calculated from the preceding statistical tests at face value. Aside from more subtle statistical tests it is wise at least to tabulate the values of $\hat{x}$ and $\sigma(\hat{x})$ periodically from all the preceding histories to ensure that the fluctuations are small enough to gain some confidence that the estimates are valid.[7]

Second, problems may be encountered where the Monte Carlo simulation gives rise to a probability density function $f(x)$ for some tally for which the variance does not exist. Then the central limit theorem is not applicable. A difficulty is that the calculation may give no obvious sign of this problem, since a finite—and totally fallacious—value of the sample variance may be calculated and used to estimate error. If the variance does not exist, then only much weaker results based on the Chebychev inequality are available for error estimates. Moreover, if a limiting distribution can be found for such a situation, it generally is not Gaussian.[4]

A third difficulty exists if the histories turn out not to be independent. This is normally not a problem in radiation transport problems, except for the criticality calculations discussed in Section 7-8.

7-5 AN EXAMPLE CALCULATION

The results of the central limit theorem are remarkable. To reiterate: even though the probability density function $f(x)$ of the sample random variable may be far from a Gaussian distribution, as is generally the case in calculating flux, current, or other particle properties, the density function $f_N(\hat{x})$ of sample mean values $\hat{x}$ is Gaussian for a sufficiently large number of N histories per batch. Moreover, the standard deviation of $f(\hat{x})$ goes in proportion to $1/\sqrt{N}$. Thus for repeated Monte Carlo calculations we may expect the resulting estimates $\hat{x}$ of $\bar{x}$ to be closely bunched around the true value provided N is sufficiently large.

To illustrate this behavior, and to demonstrate in a concrete way the behavior of some of the Monte Carlo estimators, we here analyze a very simple problem, one for which all of the relevant properties can also be obtained analyticaly. Consider a sphere of pure absorber that is one mean free path in diameter. For convenience we take the cross section as $\sigma = 1$ and ask what is the average flux in the sphere due to a uniform isotropic source emitting one neutron per second. We note that the average flux is closely related to the collision and escape probabilities for a pure absorber. The collision probability is just

$$P_c = \frac{\int dV \sigma\phi(\vec{r})}{\int dV\, S} = \frac{\overline{\sigma\phi}}{S}. \tag{7-109}$$

In our case since $\sigma = 1$ a source of one neutron per second implies that $\int dV\, S = 1$, and we have $P_c = V\bar{\sigma}\bar{\phi}$. Thus if we calculate the average flux in V, the collision probability and the escape probability,

$$P_{es} = 1 - P_c, \tag{7-110}$$

follow immediately.

In the following subsection we formulate and perform a Monte Carlo simulation of the particle transport and estimate the average flux using both collision and path length estimators. In addition to obtaining values of the sample mean and standard deviation, repeated Monte Carlo calculations are performed to illustrate the Gaussian distribution of the sample mean $\hat{x}$ about the true value. In all cases the Monte Carlo estimates are compared to existing analytical solutions. The methods used to obtain the analytical results are detailed in the final subsection.

Monte Carlo Calculations

Suppose we do a Monte Carlo simulation using both collision and track length estimators of $\bar{\phi}$. Since no scattering is present each history consists of picking an initial position and direction uniformly and isotropically; the distance to the first collision is then estimated by drawing a random number by Eq. 7-22. This is compared to the distance to the surface to determine whether the neutron collides in the sphere or escapes. For pure absorbers the collision estimator of the flux becomes binomial, since for each history, c_n in Eq. 7-50 is either 0 or 1. The path length estimator l_n in Eq. 7-54 is continuous, but it consists of only one contribution per history, the distance to the collision or to the surface, whichever is shorter.

The spherical geometry enters in choosing the distribution of source neutrons and in determining the distance to the boundary. To choose the radius r from which a particular history originates, we note that for a uniform source the probability that a neutron is born between r and $r + dr$ is proportional to the incremental volume between r and dr. The spatial probability density function is thus

$$f(r)\,dr = \frac{dV}{V} = \frac{3r^2}{R^3}\,dr. \tag{7-111}$$

Hence from Eqs. 7-7

$$F(r) = \left(\frac{r}{R}\right)^3, \tag{7-112}$$

and according to Eq. 7-18 we determine the initial radius for each neutron from a second random number ξ by

$$r = R\xi^{1/3}. \tag{7-113}$$

In this problem only the radial coordinate is required to specify the neutron's point of origin, for provided we set the $\hat{\Omega} = \hat{\Omega}(\mu, \omega)$ in the same spherical coordinates given in Chapter 1, the distance to the surface is independent of the remaining spatial coordinates. The distance is

$$y = \left[R^2 - r^2\sin^2\chi\right]^{1/2} - r\cos\chi. \tag{7-114}$$

Or, more simply,

$$y = \left[R^2 - r^2(1 - \mu^2)\right]^{1/2} - r\mu. \tag{7-115}$$

For isotropic sources, Eq. 7-115 indicates that $\mu = \cos\chi$ is evenly distributed over $-1 \ll \mu \ll 1$. Hence for each history a third random number ξ' is generated, and we take $\mu = 2\xi' - 1$. Note that there is no need to sample the azimuthal angle ω, since neither the distance to a collision nor to the surface of the sphere depends on it. Since we are to record only whether the neutron collides, and the distance to the collision, there is no need to determine the coordinates of the collision point.

A Monte Carlo computer code has been written to estimate the value of $V\bar{\phi}$. The exact values with $\sigma = 1$ are just $V\bar{\phi} = \bar{c}$ and $\bar{l}$ respectively for the collision and path length estimators. Results are given in Table 7.1 for $\hat{c}$ and $\hat{l}$ estimates with 10, 100, 1000, and 10,000 histories, along with the exact results obtained analytically.

Table 7-1 Monte Carlo Estimates of a $\bar{\phi}$ in a Purely Absorbing Sphere with $\sigma R = 1/2$

Histories N	Collision Estimator $\hat{c} \pm \sigma(\hat{c})/\sqrt{N}$	Path Length Estimator $\hat{l} \pm \sigma(\hat{l})/\sqrt{N}$
10	0.7000 ± 0.1439	0.2063 ± 0.0419
100	0.3800 ± 0.0455	0.2416 ± 0.0215
1,000	0.2810 ± 0.0143	0.2847 ± 0.0066
10,000	0.2942 ± 0.0046	0.2922 ± 0.0022
Exact[a]	$0.2927 \pm 0.455/\sqrt{N}$	$0.2927 \pm 0.2210/\sqrt{N}$

[a]Analytical solutions.

Some observations are in order. The results are not reliable for small numbers of histories, both because the central limit theorem is not applicable for small N and because the estimate of the standard deviation may be grossly in error.

For larger numbers of histories the variance of the collision estimator is larger than that of the path length estimator. This is to be expected in this problem, for $f(c)$ is a binomial density function

$$f(c) = (1 - P_c)\delta(c) + P_c\delta(c - 1), \cdot \qquad (7\text{-}116)$$

while for $\sigma R = \frac{1}{2}$, $f(l)$ is a continuous distribution over the range $0 \le l \le 1$. Moreover, as illustrated in Fig. 7-6*a* and *b*, where we have plotted respectively $f(c)$ and $f(l)$, the values of $f(l)$ are more closely bunched about the mean than those of $f(c)$. The binomial representation of Eq. 7-116 is represented in Fig. 7-6*a* by the vertical arrows at $c = 0$ and 1. Figure 7-6*b* is based on a 1000 history Monte Carlo sampling along with the analytical representation given in the following subsection.

For larger numbers of histories it is instructive to verify that the predictions of the central limit theorem hold for our Monte Carlo calculation. To this end 500 batches of 25 histories each were tabulated, and in Fig. 7-7*a* and *b* are shown histograms of the distributions of sample mean values $f_{25}(\hat{c})$ and $f_{25}(\hat{l})$, as well as the Gaussian distributions predicted by the central limit theorem; in the latter, the exact values of the mean and variance are used. The close approximations of the histograms to the Gaussian curves is evident, indicating that for this particular problem the central limit theorem predicts the distribution quite well even though the number of histories per batch, $N = 25$, is very small.

Using these figures we have a more complete picture with which to view the properties of the estimators. Clearly the path length estimator results in smaller errors than the collision estimator for a given number of histories. This stems from the smaller spread of l about $\bar{l}$ than of c about $\bar{c}$, as illustrated in Fig. 7-7. Moreover, by looking at the definition of the mean it is clear that the best estimator of all would have the form $f(x) = \delta(\bar{x} - x)$, for then there would be zero variance. Of course such an estimator is not available. In general, however, we would like to have estimators that result in nearly all histories making comparable contributions, for this leads to $f(x)$ that is concentrated about $\bar{x}$ with a resulting small variance.

Analytical Solution

The foregoing pure absorber problem is for illustration only, since it is sufficiently simple that all of the results may be obtained exactly by

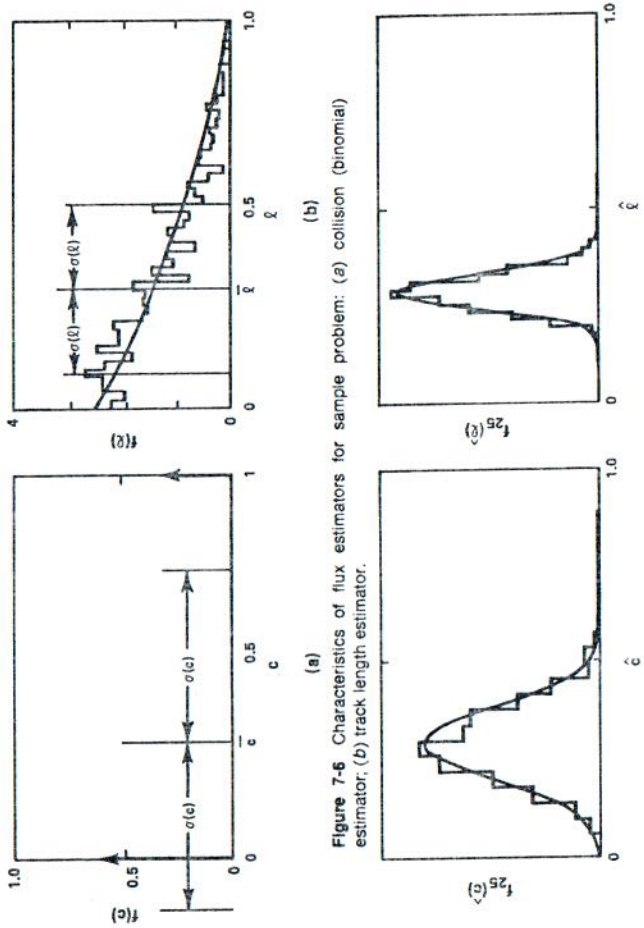

Figure 7-6 Characteristics of flux estimators for sample problem: (*a*) collision (binomial) estimator; (*b*) track length estimator.

Figure 7-7 Distribution of average flux estimates with 25 histories / calculation: (*a*) collision estimator; (*b*) track length estimator.

analytical methods. In Eq. 7-44 we have already obtained the conditional probability density function that a neutron will travel a distance between l and $l + dl$ in a solid, given a distance y to the surface:

$$f(l|y) = \sigma e^{-\sigma l} H(y - l) + e^{-\sigma y}\delta(l - y). \tag{7-117}$$

From Eq. 7-42 it is clear that the probability that such a particle will collide in the volume is

$$P_c(y) = 1 - e^{-\sigma y}. \tag{7-118}$$

If we know the density distribution $h(y)$ of path lengths y to the surface produced by a given source distribution for a solid of given size and shape, then the collision probability is

$$P_c = \int_0^\infty dy\,(1 - e^{-\sigma y})h(y), \tag{7-119}$$

from which the probability density function for the collision estimator given in Eq. 7-116 can immediately be determined. Since $f(c)$ is a binomial estimator, from Eq. 7-76 we have

$$\sigma^2(c) = P_c(1 - P_c). \tag{7-120}$$

The probability density distribution for the path length estimator can be obtained by integrating $f(l|y)$ over the distribution of path lengths:

$$f(l) = \int_0^\infty dy f(l|y)h(y). \tag{7-121}$$

And then

$$\sigma^2(l) = \int_0^\infty dl\, l^2 f(l) - \left[\int_0^\infty dl\, l f(l)\right]^2. \tag{7-122}$$

For solids of very elementary shapes, the distributions $h(y)$ of distances to the surface have been obtained elsewhere for sources that are uniform and isotropic.[17] In particular, for a sphere of radius R,

$$h(y) = \begin{cases} \dfrac{3}{4R}\left(1 - \dfrac{y^2}{4R^2}\right), & y < 2R, \\ 0, & y > 2R. \end{cases} \tag{7-123}$$

Combining this expression with Eq. 7-119 thus yields for the collision probability

$$P_c = 1 - \frac{3}{8(\sigma R)^3}\left[2(\sigma R)^2 - 1 + (1 + 2\sigma R)e^{-2\sigma R}\right]. \tag{7-124}$$

Again using $h(y)$ in Eq. 7-121, we obtain the path length distribution to be

$$f(l) = \sigma e^{-\sigma l}\left[1 + \frac{3}{4\sigma R} - \frac{3l}{4R} - \frac{3}{16}\frac{l^2}{\sigma R^3} + \frac{l^3}{16R^3}\right], \tag{7-125}$$

which is plotted for $\sigma R = \frac{1}{2}$ in Fig. 7-6*b*. The variance for the path length estimator is obtained by combining this equation with Eq. 7-122.

7-6 NONANALOG MONTE CARLO

Properties of Variance

The foregoing simple problem leads to two extreme forms of estimators: binomial sampling in which particle contributions to the result are either zero or one, and estimators in which all particle histories make a nonzero contribution to the result. In more realistic problems, simple binomial sampling is rarely used. Neither is it usually possible to find an estimator in which all histories make a nonzero contribution. Estimators are likely, rather, to have both a delta function and a continuous contribution of the form[7]

$$f(x) = c\delta(x - 0) + g(x), \tag{7-126}$$

where one must have from Eqs. 7-4 and 7-65,

$$\int_{-\infty}^{\infty} dx\, g(x) = 1 - c \tag{7-127}$$

and

$$\bar{x} = \int_{-\infty}^{\infty} dx\, x g(x). \tag{7-128}$$

The relationship of these quantities is sketched in Fig. 7-8. The delta function term comes from particles that contribute nothing to the result while the second term $g(x)$ indicates the spread in path lengths or other

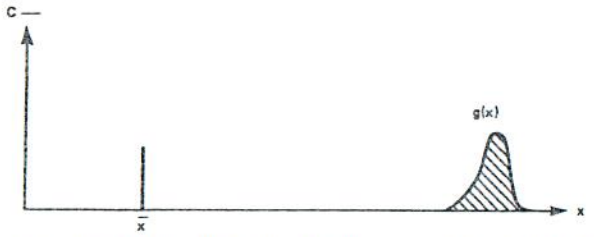

Figure 7-8 Tally distribution for a problem in which a fraction (1-c) of the y histories contribute to the result.

characteristics of the particles that do contribute. Such situations occur, for example, in shielding calculations where a large fraction c of the particles never penetrate to the outside of the shield where the flux is to be calculated. Correspondingly, those particles that do reach the area of interest make varying nonzero contributions, depending on their position, direction and energy.

The contribution to the statistical uncertainty of the result $\bar{x}$ for Fig. 7-8 can be split into two parts since the variance of $f(x)$ can be written as the sum of the contributions of the two terms:

$$\sigma^2(x) = \sigma_{\text{eff}}^2 + \sigma_{\text{int}}^2. \tag{7-129}$$

The first term σ_{eff} is due to the inefficiency of the Monte Carlo procedure. That is to say that not all of the particles contribute to the result. The second contribution σ_{int} is the variance that is intrinsic to the spread of nonzero values of contributing histories about $\bar{x}$.

For many realistic problems the value of c is unacceptably large when the analog Monte Carlo methods are used, even when the best available estimators for a particular quantity are used. To take an extreme example, suppose that a shield provides an attenuation of about 10^6. Then only one analog particle per million will contribute to $g(x)$ above! Because of the pervasiveness of this problem it is necessary to depart from analog Monte Carlo in order to reduce the variance of the result, particularly by increasing the fraction of histories that contribute to the result.

In doing this, however, a tradeoff is encountered. As various nonanalog devices are applied to reduce the variance, the computing time per history is likely to increase. Therefore, some figure of merit is needed to determine whether a net gain in accuracy for a given computing time has been achieved. The following criterion is frequently used. Suppose we take the

variance of the result $\sigma^2(\hat{x})$ as a measure of the inaccuracy, and the total computer time T as a measure of the computational effort. Then a reasonable figure of merit is the inverse of $\sigma^2(\hat{x})T$. Then letting $T = Nt$ where t is the mean time per history, and recalling that $\sigma^2(\hat{x}) \approx \sigma^2(x)/N$ we have for the figure of merit

$$\frac{1}{\sigma^2(x)t}. \tag{7-130}$$

In what follows some of the techniques that are discussed actually cause an increase in σ^2. However, if in such cases they also cause a large reduction in the time per history, they will increase the figure of merit, and therefore their use is advantageous.

Importance Sampling

The problem of reducing the statistical uncertainty of Monte Carlo results may be approached in a somewhat more formal manner through the concept of importance sampling.[1,5,18] The object of a Monte Carlo calculation is to calculate a mean value

$$\bar{x} = \int x f(x)\, dx, \tag{7-131}$$

where x is some random property (variable) of the neutron history. The variance

$$\sigma^2(x) = \int (x - \bar{x})^2 f(x)\, dx \tag{7-132}$$

is a measure of the uncertainty.

Suppose we now modify our Monte Carlo procedure such that we sample not $f(x)$ but some modified probability density function, say $\tilde{f}(x)$. Then if we define a weight function

$$w(x) = \frac{f(x)}{\tilde{f}(x)}, \tag{7-133}$$

Eq. 7-131 may be written as

$$\bar{x} = \int x w(x) \tilde{f}(x)\, dx. \tag{7-134}$$

Thus if we are to obtain an unbiased modification, the value of $\bar{x}$ must be preserved. This is done by sampling from $\tilde{f}(x)$ and weighting the result by

$w(x)$. For our N histories we started out by tallying

$$\hat{x} = \frac{1}{N}\sum_n x_n \tag{7-135}$$

from the sample of $f(x)$. Now we tally

$$\widehat{(wx)} = \frac{1}{N}\sum_n w(x_n)x_n \tag{7-136}$$

by sampling $\tilde{f}(x)$ for the x_n. If the sampling of $f(x)$ and of $\tilde{f}(x)$ is unbiased, both $\hat{x}$ and xw have an expectation value of $\bar{x}$; hence they converge to $\bar{x}$ as the number of histories goes to infinity.

The objective of the foregoing exercise is to obtain an estimator with a smaller variance and therefore a smaller statistical uncertainty. The variance of $xw(x)$ is

$$\sigma^2[xw(x)] = \int [xw(x) - \bar{x}]^2 \tilde{f}(x)\,dx \tag{7-137}$$

or, using Eq. 7-134 and the fact that $\tilde{f}(x)$ is a probability density function, and hence $\int \tilde{f}(x)\,dx = 1$, we have

$$\sigma^2[xw(x)] = \int x^2 w(x)^2 \tilde{f}(x)\,dx - \left[\int xw(x)\tilde{f}(x)\,dx\right]^2. \tag{7-138}$$

The associated sample variance is then

$$S^2 = \frac{N}{N-1}\left[\widehat{(wx)^2} - \widehat{(wx)}^2\right], \tag{7-139}$$

where

$$\widehat{(wx)^2} \equiv \frac{1}{N}\sum_n w(x_n)^2 x_n^2. \tag{7-140}$$

Hence if we can reduce the sample variance without altering $\bar{x}$, we are successful. In a particular instance if we choose $\tilde{f}(x)$ such that

$$w(x)x = \bar{x}, \tag{7-141}$$

we have obtained a zero variance result, and therefore one with no statistical uncertainty. The fulfillment of Eq. 7-141, however, requires that we solve the adjoint transport equation to determine $w(x)$ to meet this condition. As discussed in Chapter 1, the solution of this equation is just as difficult as the

solution of the transport equation itself. Therefore, in a practical sense there are no zero variance sampling methods. However, the very knowledge of the existence of such a function leads one to attempt approximations to it that reduce variance without leading to undue increases in computation time per history. Methods have been developed in which approximate solutions of the adjoint equations are used to reduce the variance of a Monte Carlo calculation.[19] Such approximate methods often are based on discrete ordinates or other deterministic methods in simplified geometries. While the use of deterministic methods to reduce variance through importance sampling or related controlled variants [1-3] techniques can be quite powerful in some circumstances, a detailed discussion would carry us too far afield. We concentrate our attention instead on those variance reduction techniques that are more universally applied to the extent that they are incorporated into nearly all Monte Carlo codes.

Variance Reduction Methods

Other than devising improved estimators, most variance reduction devices require that we modify the simulation of the particle histories in a nonanalog manner. The goal, again stated in terms of Figure 7-8, is to increase the fraction of particles that contribute to the result, thus decreasing the delta function at zero and moving the contributing distribution closer to the mean value $\bar{x}$. This task is carried out as follows.

Nonanalog procedures are most frequently applied at each collision, boundary crossing, or other event during a particle history. Thus the particle weight must be appropriately adjusted each time that such an event takes place to compensate for the modified sampling. Suppose for the nth particle that $x_{n1}, x_{n2}, \ldots, x_{ni}$, are collisions, track lengths, or other tallies that contribute to the sample mean. If we designate $w_{n1}, w_{n2}, \ldots, w_{ni}$, as the nth particle weights at the times that these tallies are made, then the contribution of the nth particle to the sample mean and variance, Eqs. 7-136 and 7-139 respectively, is determined from

$$w(x_n)x_n = \sum_i w_{ni}x_{ni}, \tag{7-142}$$

where for $i > 0$,

$$x_n = \sum_i x_{ni} \tag{7-143}$$

and

$$w(x_n) = \frac{1}{x_n}\sum_i w_{ni}x_{ni}. \tag{7-144}$$

The foregoing procedure is made clear below by the detailed discussion of several of the standard variance reduction techniques. Some of these are often referred to as biasing techniques. It must be kept clearly in mind, however, that only the probability density function is biased; the tally procedure must also be modified to maintain an unbiased estimator of the mean.

Absorption Suppression. A nearly universal option of Monte Carlo codes is that a particle history is not terminated by absorption. This often is called survival biasing or implicit capture. In it, once the location and energy of a scattering event are specified, the criterion $\xi > \sigma_a/\sigma$ is no longer used to determine whether the particle will survive the collision. Rather, the weight of the particle at the ith collision is reduced by setting

$$w_{n,i+1} = w_{ni} \cdot \left(1 - \frac{\sigma_a}{\sigma}\right) \tag{7-145}$$

to correspond to the survival probability. This procedure lengthens the computing time per history, since the number of collisions is increased. This is more than offset, however, by the reduction in variance, provided one of the following criteria for history termination is used.

History Termination and Russian Roulette. If absorption is suppressed, then the only way for a history to terminate is by leaking from the system. If the characteristic dimensions of the system are large in terms of mean free paths, this will lead to very inefficient sampling. For after a sufficient number of collisions the particle weight will be so small that it no longer will be capable of contributing significantly to the tallies. Therefore, a supplementary nonanalog method is normally included to terminate the history if the weight becomes too small. Setting some lower limit on the weight and terminating the history when the weight becomes less than the limit is one possibility. However, this will cause the tallies to be underestimated, and the resulting bias may be significant. More physically justifiable criteria may be used to terminate histories. For example, in shielding problems it is often only the neutrons or gamma rays above some energy threshold that can contribute significantly to the result. In this case, histories may be terminated when the particles scatter to energies below such a threshold.

Since it introduces no bias, Russian roulette is normally considered a more reliable method for terminating histories. In this procedure one first checks to see if the particle weight has fallen below some minimum value. A uniformly distributed number $0 \le \xi \le 1$ is generated and compared to an input number Ξ, where Ξ might be typically between 2 and 10. If $\xi > 1/\Xi$,

the history is terminated. If $\xi \le 1/\Xi$, the history is continued with a weight multiplied by a factor of Ξ. In general, Russian roulette increases the variance of the result. Since the further tracking of unimportant particles is eliminated, however, the average computation time per history is reduced. Moreover, if reasonable values of the cutoff weight and of Ξ' are chosen, the net effect should be an increase in the figure of merit $1/(t\sigma^2)$, given by Eq. 7-130.

Splitting and Russian Roulette. When particles become unimportant, for example, due to their small weight, we may play Russian roulette in order to decrease the number of particles that must be tracked further while increasing the weight of those remaining to retain unbiased estimators. Similarly, if particles become very important, it is often found advantageous to increase their number by splitting them into two or more particles, each with an appropriately reduced weight to maintain unbiased estimators. If we have a Ξ-to-one splitting of a particle, each of the new particles will have only $1/\Xi$ of the original particle weight. Splitting reduces the variance of the results but causes computation time per each initiated history to increase. The important point is that when effectively used, splitting, like Russian roulette, causes a net increase in the figure of merit, $1/(t\sigma^2)$.

The effect on computation time per history of these converse procedures is obvious. The effect on variance is more subtle, but it may be understood in terms of the probability density function in Fig. 7-8. When Russian roulette is applied to small weight particles, contributions are added to Fig. 7-8 at $x = 0$, from terminated histories, and at large values of x, well above the mean. Thus Russian roulette causes a spread in the density distribution $f(x)$ further from $\bar{x}$ and thereby increases the variance. Conversely, splitting has the effect of creating a larger contribution to $f(x)$ at smaller values of x, which are closer to the mean. Thus the variance is reduced.

Splitting most commonly is made to take place at boundary crossings. This is illustrated in the deep penetration problem shown schematically in Fig. 7-9. In this problem the object is to determine the fraction of the particles entering on the left that penetrate to the right-hand side of the shield. If the shield is many attenuation lengths thick, then on the average only a small fraction of the particles will penetrate.

In Fig. 7-9, the problem domain is divided into a number of subdomains as indicated by the dashed lines. For this problem the particles will have increased importance as one moves from left to right. For simplicity assume that all of the values I_{i+1}/I_i are integers greater than one. Then, when a particle crosses a boundary to the right it is replaced by I_{i+1}/I_i particles, each with a weight of I_i/I_{i+1} of the original particle's weight. Each of the new particles is then tracked, generating independent sets of random numbers for collisions, path lengths, and so on.

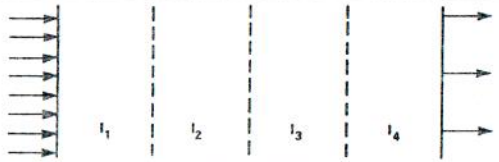

Figure 7-9 A deep penetration problem divided into four regions for splitting.

Conversely, if a particle moves to the left from a region with importance I_{i+1} to I_i, Russian roulette is played with $\Xi = I_{i+1}/I_i$ to terminate selectively some of the relatively unimportant particle histories. In using geometrical splitting and Russian roulette in conjunction with Eqs. 7-136 and 7-139 for estimating mean and variance values, all of the progeny of a source particle must be included under x_n. Otherwise the correlated behavior of the progeny might cause the variance to be seriously underestimated.

The foregoing splitting procedure may be generalized to three-dimensional regions and to noninteger values of the importance ratio. In general, it is a very effective method of variance reduction for deep penetration problems, particularly if one has either some intuition or an approximate adjoint result from which to make good selections of the importance regions.

Geometry splitting with Russian roulette is a reliable variance reduction technique because it causes the particle weight to have more nearly the same values within a given volume. Splitting or Russian roulette could be used separately; however, the variance then will be larger than when both are used together, since the weights will have a wider spread of values within a cell.

Experience has indicated that the best splitting results are obtained for deep penetration problems when the number of particles passing through the system is kept approximately constant.[7] Thus in the foregoing illustration one might do a two-for-one splitting wherever the particle population has dropped by a factor of 2. Large splitting ratios (e.g., 20 to 1) can be used to build up the population of penetrating particles after it has been substantially attenuated. However, this will not regain information from the lost particles, and in general it will place a heavy burden on reliable sampling due to the correlation of progeny of the same starting particle.

The Exponential Transformation. As an alternative to splitting, the exponential transformation prevents the rapid deterioration of particle population in deep penetration problems by stretching the distance between collisions in the forward direction in an unbiased manner. Particles are

allowed to move in a preferred direction by artificially reducing the macroscopic cross section in that direction.[20]

Suppose the particles are to move preferentially in the x direction. Then we take as a transformed cross section

$$\sigma_{ex} = \sigma_t(1 - p\hat{\Omega} \cdot \hat{\imath}), \tag{7-146}$$

where the degree of biasing is determined by the parameter $0 \le p < 1$. At a collision the particle weight is multiplied by a factor w_{ex} to preserve the expected weight. This weight is determined by first noting that the probability of colliding between travel distances u and $u + du$ is $\sigma \exp(-\sigma u)\, du$ regardless of whether $\sigma = \sigma_t$ or $\sigma = \sigma_{ex}$. Hence to preserve the expected weight of the collided particle one must have

$$\sigma_t e^{-\sigma_t u}\, du = w_{ex}\sigma_{ex} e^{-\sigma_{ex} u}\, du \tag{7-147}$$

Combining Eqs. 7-146 and 7-147 we then have

$$w_{ex} = \frac{\exp(-p\sigma_t \hat{\Omega} \cdot \hat{\imath} u)}{1 - p\hat{\Omega} \cdot \hat{\imath}}. \tag{7-148}$$

A different correction must be made if the particle reaches a boundary before collision. Then the weight must be modified so that it is multiplied by the probability that the particle reaching the surface remains constant:

$$e^{-\sigma_t u} = w_{ex} e^{-\sigma_{ex} u}. \tag{7-149}$$

Thus

$$w_{ex} = \exp(-p\sigma_t \hat{\Omega} \cdot \hat{\imath} u). \tag{7-150}$$

Some precautions are also in order in applying the exponential transform. As an example, for one-dimensional penetration problems in highly absorbing media the variance will decrease as p is increased above zero until some optimal value, say $\tilde{p}$, is reached. Thereafter the variance will increase as p increases toward one. Choosing a reasonable value of p is a matter of experience. It should be pointed out, moreover, that choosing parameters for the transform can be very tricky in multidimensional problems, and that if any mechanism for particle termination is used, it must be compatible with the exponential transform.

Forced Collisions. In contrast to the exponential transform, where the distances between collisions is modified, a method is needed whose object is

to shorten the distance between collisions.[4] Such an artifice is most useful in situations where a reaction rate or other quantity is to be calculated over a small volume. For such situations it is often necessary to modify analog Monte Carlo to increase the number of collisions in the volume. Otherwise, the small number of collisions would lead to inadequate statistics.

In the method of forced collisions we split a particle into two smaller weight particles, the first of which passes through the volume without colliding, and the second of which is forced to collide. Suppose that a particle with weight w enters a volume such that it must travel a distance u before exiting from the volume. The probability that it will pass through the volume without collision is then $\exp(-\sigma u)$, where σ is the total cross section. We thus divide our particle into two particles. The particle that survives without collision has a weight

$$w_e = we^{-\sigma u}, \tag{7-151}$$

and the particle that collides has a weight

$$w_c = w(1 - e^{-\sigma u}). \tag{7-152}$$

The surviving particle history then is continued with its modified weight, by sampling to find how far from its position on the surface of the volume it will travel before making its next collision. The position of the collision of the particle with weight w_c within the cell also must be found within the cell. The probability density function for collision of this particle within the cell is

$$f(x) = \frac{\sigma e^{-\sigma x}}{1 - e^{-\sigma u}}, \qquad 0 \le x \le u. \tag{7-153}$$

Hence using Eqs. 7-7 and 7-17 we generate x, the distance traveled before a collison from the random number ξ to be

$$x = -\frac{1}{\sigma}\ln\{(1 - \xi(1 - e^{-\sigma u})\}. \tag{7-154}$$

Once the point of collision is determined, the history is followed with reduced weight w_c by next applying collision mechanics sampling to determine direction, energy, and weight of the scattered particle.

Forced collisions in small volumes are likely to lead to small weight particles being generated. Russian roulette or other weight cutoff mechanisms, however, are normally not used in that volume. For only then can one ensure that the collided sample that was obtained through forced collision will not be terminated.

Source Biasing. In source biasing we distort the distribution of source particles in order to produce more of them in regions of the space-angle-energy phase space that are known to be most important for the result. Suppose we replace a source distribution $S(\vec{r}, E, \hat{\Omega})$ by a biased distribution $S'(\vec{r}, E, \hat{\Omega})$. If each particle from the unbiased distribution were to have a weight of 1, then in order to preserve the unbiased estimators we would need an initial weight of

$$w = \frac{S(\vec{r}, \hat{\Omega}, E)}{S'(\vec{r}, \hat{\Omega}, E)} \tag{7-155}$$

for a particle born at $\vec{r}, \hat{\Omega}, E$.

An example of source biasing may be helpful. In shielding from fission sources it is well known that neutrons of about 8 MeV contribute most to the radiation doses,[21] even though the average fission neutron energy is only about 2 MeV. Hence one might want to have a value of S'/S that is greater than 1 for neutrons with energies greater than say 5 MeV, and decreasing rapidly as the neutron energies fall below this value.

Correlated Sampling. In problems where one is attempting to measure a small perturbation of a system, the perturbation usually will be masked by the statistical errors if an attempt is made to calculate the change as the difference between two independent (i.e., uncorrelated) Monte Carlo results. This situation can be alleviated by correlated sampling.[22] Two Monte Carlo runs are made in which the corresponding histories are initiated and followed using the same set of pseudo random numbers. The sequence of events for the perturbed and unperturbed runs are hence identical until the perturbation causes the histories to differ. Hence for no perturbation, identical results are obtained for the two runs. In the presence of the perturbations, the results differ only by the amount that the perturbation causes the histories to diverge.

Optical Reciprocity. The optical reciprocity relations discussed specifically in conjunction with the calculation of collision probabilities in Chapter 5 can be applied more generally as a variance reduction technique in Monte Carlo calculation. For often the reciprocal problem solution will have an inherently smaller variance than the original problem. This is particularly true when one is trying to calculate a flux, detector response, or other reaction rate over a small volume. We illustrate with the following simple monoenergetic example.

Suppose we have an isotropic source distribution $S(\vec{r})$ in a solid with vacuum boundary conditions. We want to calculate the flux integral

$$\int_{V_d} dV \phi(\vec{r}) \tag{7-156}$$

over a small detector volume V_d in the much larger volume V. This is a difficult Monte Carlo problem, for very few neutrons will collide or even pass through the small volume V_d, making both collision and path length estimators very inefficient. Suppose we call this Problem 1 and consider a reciprocal Problem 2 also in the same solid with vacuum boundary conditions. The reciprocity relationship, Eq. 5-155, then reduces to

$$\int dV \int d\Omega \, \psi_2(\vec{r}, -\hat{\Omega}) q_1(\vec{r}) = \int dV \int d\Omega \, \psi_1(\vec{r}, \hat{\Omega}) q_2(\vec{r}), \tag{7-157}$$

since at the boundary we have

$$\psi_1(\vec{r}, \hat{\Omega}) = 0 \quad \text{and} \quad \psi_2(\vec{r}, \hat{\Omega}) = 0, \qquad \vec{r} \in \Gamma, \hat{\Omega} \cdot \hat{n} < 0 \tag{7-158}$$

and hence the surface terms vanish. Now suppose for our reciprocal problem we take

$$q_2(\vec{r}, \hat{\Omega}) = \begin{cases} 1, & \vec{r} \in V_d, \\ 0, & \vec{r} \notin V_d. \end{cases} \tag{7-159}$$

Carrying out the integrals we obtain from Eq. 7-157

$$\int_V dV \phi_2(\vec{r}) q_1(\vec{r}) = \int_{V_d} dV \phi_1(\vec{r}). \tag{7-160}$$

From this relationship we see that if we solve for a weighted integral of $\phi_2(\vec{r})$ over the entire volume, we can set this equal to our integrated detector flux. This is a much lower variance calculation to carry out. We simply track neutrons that originate from the localized source in V_d and nearly all of them will contribute to the weighted flux integral on the left of Eq. 7-160, since it includes the entire problem domain.

The foregoing procedure may be taken one step further to estimate the flux at a point. Suppose instead of Eq. 7-159 we take $q_2(\vec{r}, \hat{\Omega}) = \delta(\vec{r} - \vec{r}_d)$; then $\phi_1(\vec{r})$ in the above equation becomes $\phi_1(\vec{r}_d)$, the flux at $\vec{r}_d$. Such applications of optical reciprocity are very useful, except where the source $q_1(\vec{r})$ is also localized over a small volume, for then the estimation of the left-hand side of Eq. 7-160 may be no less difficult than that of the right.

For general-purpose Monte Carlo calculations tracking must be done in a phase space that includes energy as well as space and angle. Optical reciprocity in the form we have discussed thus far is no longer applicable. One must rather form the reciprocal problem with the adjoint transport equation, and Eq. 7-160 must be replaced by a more general energy-dependent expression in which $\phi_2(\vec{r})$ corresponds to the adjoint flux. Powerful applications of such adjoint Monte Carlo methods may be found in the literature.[2, 13, 23]

7-7 TRACKING IN PHASE SPACE

In the foregoing discussions of both analog and nonanalog Monte Carlo methods very little was said either about the detailed mechanics of collisions or about the tracking of particle paths through complicated spatial configurations. This has been deliberate in order not to obscure the fundamental concepts with an excess of detail. It is the ability to handle the details of energy-dependent cross sections and collision mechanics, and to track particles through bodies of complex shapes and orientations, however, that provides Monte Carlo its primary advantage relative to deterministic methods. In this section we sketch some of the techniques used in collision mechanics. Our treatment is limited, for taken too far afield, it entangles us in the details of how nuclear cross section sets are generated and handled. We then discuss the tracking mechanisms used to follow particles through space and across material interfaces in complex geometrical configurations. Ultimately such discussions become involved in the details of the geometry tracking packages that are incorporated into particular Monte Carlo codes.

Cross Sections and Collisions

In considering the treatment of the energy variable, one must first distinguish between continuous energy and multigroup Monte Carlo. In continuous Monte Carlo, cross section data are stored either in the form of tables or analytical models so that when a particle makes a collision at energy E the cross sections can either be evaluated directly or interpolated to whatever level of accuracy is desirable. The same holds true for scattering functions. Thus in principle no physical approximations are necessary in the treatment of the nuclear data, and the accuracy of the resulting Monte Carlo calculation is limited only by errors in the data and the statistical uncertainty due to the finite number of histories. Such calculations are particularly useful for benchmarking more approximate methods.

In contrast, multigroup Monte Carlo[6] simulates not the exact transport equation but the discrete energy approximation derived in Chapter 2. Thus the systematic errors incurred in the generation of the multigroup cross sections are present also in the subsequent Monte Carlo results. Multigroup Monte Carlo is nevertheless a very useful tool, for it can be used to check the angular approximations and geometrical modeling of deterministic methods. More important, it can be combined with discrete ordinates or other deterministic methods using the same cross section sets.

There are significant differences in the way neutron and photon cross section data are treated in continuous Monte Carlo codes. These stem primarily from the fact that photon information is a rather smooth function of energy, and moreover varies continuously with the atomic charge of the nucleus. In contrast, the resonance structure of neutron cross sections causes rapid variation in energy, while at the same time making it impossible to infer the cross section of one nuclide from those of adjoining nuclides on the periodic table. The result is that while photon cross sections can be generated from relatively coarse mesh energy and atomic number interpolation, much more detailed tables of data are needed for each nuclide with which a neutron may collide.

Neutron Scattering. As an example of how a collision simulation might work in a continuous energy Monte Carlo code assume that a neutron is traveling through a medium with energy E in direction $\hat{\Omega}$. To obtain a collision site from Eq. 7-22 the mean free path and therefore the total macroscopic cross section $\sigma(E)$ for the material composition of the medium must be obtained from the data tables. Once the site of the collision has been obtained, the neutron weight may be multiplied by $[\sigma(E) - \sigma_a(E)]/\sigma(E)$ and the absorptions tallied. Another random number is generated, and the nuclide with which the neutron is to scatter is determined by comparing that number with the ratios of $\sigma_s^i(E)/\sigma_s(E)$, where σ_s^i is the scattering cross section of the ith nuclide. If more than one type of scattering is present (e.g., elastic and inelastic), the ratios σ_n^i/σ_s^i and $\sigma_{n'}^i/\sigma_s^i$ are compared to the random number to determine which type of scattering takes place.

Once the nuclide and type of scattering have been specified, we are prepared to determine the particle energy and direction, E' and $\hat{\Omega}'$, following the scattering event. We first consider the case of elastic scattering, where μ_{cm}, the cosine of the scattering angle in the center of mass system, is first sampled. If the scattering is isotropic in the center of mass system, then μ_{cm} is determined by sampling a uniform probability density function over the interval $-1 \le \mu_{cm} \le 1$. If the center-of-mass scattering is anisotropic,

then a table look-up or analytical model of the scattering law must be used in sampling μ_{cm}.

Once μ_{cm} has been specified, conservation of energy and momentum arguments determine the energy after collision to be[24]

$$E' = \frac{E(A^2 + 2A\mu_{cm} + 1)}{(A+1)^2}, \tag{7-161}$$

where A is the atomic mass. With E' determined, the cosine of the scattering angle in the laboratory system may be shown to be

$$\cos\theta \equiv \hat{\Omega} \cdot \hat{\Omega}' = \frac{1}{2}(A+1)\sqrt{\frac{E}{E'}} + \frac{1}{2}(A-1)\sqrt{\frac{E'}{E}}. \tag{7-162}$$

Finally, knowing $\cos\theta$, we must specify a polar angle ω before the direction $\hat{\Omega}'$ can be determined. Since the scattering law is independent of ω, we simply sample $\omega = 2\pi\xi$, where ξ is a uniformly distributed random number. Then it may be shown that the direction cosines of $\hat{\Omega}'$ are given in terms of those of $\hat{\Omega}$ by[4]

$$\begin{aligned}
\Omega_x' &= \frac{\sin\theta}{\sqrt{1-\Omega_z^2}}\left[\Omega_y \sin\omega - \Omega_y\Omega_x\cos\omega\right] + \Omega_x\cos\theta, \\
\Omega_y' &= \frac{\sin\theta}{\sqrt{1-\Omega_z^2}}\left[-\Omega_x\sin\omega - \Omega_z\Omega_y\cos\omega\right] + \Omega_y\cos\theta, \\
\Omega_z' &= \sin\theta\sqrt{1-\Omega_z^2}\cos\omega + \Omega_z\cos\theta.
\end{aligned} \tag{7-163}$$

The procedure for inelastic scattering by the nucleus is somewhat more complicated. One must first sample a nuclear model to determine the excitation energy E^* of the residual nucleus; both effective temperature models and discrete energy level look-ups may be used for this purpose. In the limit where the atomic weight is large, $A \gg 1$, the scattering will be isotropic in the laboratory system, allowing Eqs. 7-38 to be used in conjunction with Eqs. 7-163 to determine the new particle direction $\hat{\Omega}$. For this situation we then have

$$E' = E - E^*. \tag{7-164}$$

In the cases where nuclear inelastic scattering is significant in lighter nuclei generalizations of Eqs. 7-161 and 7-162 are developed in detail

elsewhere[21, 25] for the determination of $\hat{\Omega}'$ and E' once E^* has been determined. Likewise if scattering of thermal energy neutrons is to be considered one of the several models taking into account, both the thermal motion of the target nuclide and possibly the chemical binding of the nuclide must be utilized. Such formulations are discussed elsewhere.[5]

Photon Interactions. If low-energy photon transport is simulated by Monte Carlo methods, a number of phenomena that are not important at higher energies must be included: photoelectric fluorescence, coherent Thompson scattering, and form factors from binding in Compton scattering.[7] Here we limit consideration to higher energy photon transport such as that encountered in gamma ray shielding problems. In this case the cross section may be considered to consist of only three contributions: photoelectric effect, Compton scattering, and pair production:

$$\sigma(E) = \sigma_{pe}(E) + \sigma_{cs}(E) + \sigma_{pp}(E). \tag{7-165}$$

The photoelectric effect is treated as an absorption reaction, while the Compton scattering and pair production are treated as scattering reactions. Typically absorption is suppressed by reducing the photon weight by $(1 - \sigma_{pe})/\sigma$ and then a random number is generated and compared to the ratio $\sigma_{cs}/(\sigma_{cs} + \sigma_{pp})$ to determine whether Compton scattering or pair production has taken place. In contrast to neutron interactions no distinction need be made as to which nuclide is the target.

Pair production is a threshold cross section with nonzero values only above 1.022 MeV. It is typically modeled as follows. The photon vanishes, and the resulting positron is assumed to be annihilated by an electron at the collision point producing two gamma rays, isotropically distributed in the laboratory system, each with an energy of 0.511 MeV. Typically this is treated by producing only one 0.511 MeV photon, and multiplying the weight by 2.[7] Hence the number of photons that must be tracked is not doubled with each pair production collision.

For gamma rays, binding effects can be neglected and Compton scattering considered for free electrons. In this situation the Klein–Nishina formula and the Compton law can be combined to yield the density function for the conditional probability that a photon with energy E will scatter through an angle whose cosine is μ in the laboratory system[21]

$$f(\mu|E) = \frac{\pi r_0^2}{\sigma_e(E)}[1 + E(1-\mu)]^{-2}\left[E(1-\mu) + \mu^2 + \frac{1}{1 + E(1-\mu)}\right], \quad -1 < \mu \le 1. \tag{7-166}$$

Here $\sigma_e(E)$ is the Compton scattering cross section per electron, r_0 is the classical electron radius, and E is given in units of the electron rest mass energy, 0.511 MeV. Once Eq. 7-166 is used to determine $\mu = \cos\theta$, the scattering angle, the polar angle ω through which the photon scatters can be chosen from a uniform distribution; and then Eqs. 7-163 may be applied to determine the new direction $\hat{\Omega}'$ of photon energy. The photon energy following the collision is then given by the Compton scattering law

$$E' = \frac{E}{1 + E(1-\mu)},$$

where the energies are again given in units of the electron rest mass.

Multigroup Interactions. The foregoing collision mechanics procedures for both neutrons and photons are modified significantly when multigroup Monte Carlo is used. Absorption is again suppressed by particle weight reduction. One must then determine the group and the direction of the particle after the scattering collision. Suppose a particle scatters in group g of G energy groups. To determine the group g' into which it scatters a random number ξ is generated. If

$$\frac{\sum_{g''=1}^{g'-1} \sigma_{g''g}}{\sum_{g''=1}^{G} \sigma_{g''g}} \le \xi \le \frac{\sum_{g''=1}^{g'} \sigma_{g''g}}{\sum_{g''=1}^{G} \sigma_{g''g}}, \tag{7-167}$$

the particle is emitted in group g'. If scattering is isotropic, then μ and ω are uniformly distributed. If not, the angular distribution of scattered particles usually is represented in terms of the laboratory scattering cosine μ, by a low-order Legendre series. This may be sampled to determine μ. The azimuthal angle ω is then uniformly sampled and the final direction determined.

Tallies

The tallying procedures, as well as the collision mechanics, must be generalized to take into account the energy of the particle and the nonanalog tracking procedures. If we are to determine the average flux in some volume $\bar{V}$, which we assume is uniform, then

$$\bar{\phi} = \int dE \int dV \phi(\vec{r}, E). \tag{7-168}$$

Comparing this expression with the path length estimator given by Eq. 7-52 we see that the estimator retains the same form insofar as the energy dependence is concerned. The only exception is in the situation where the integral in Eq. 7-168 does not include all energy. In that case only path lengths of particles within the specified energy interval are included. Likewise, the current and surface crossing estimators of Eq. 7-59 and 7-60 require no other modifications. The tallying of the collision estimator, Eqs. 7-51, must be modified due to the energy dependence of the cross section in the denominator. In nonanalog tracking each particle is assigned a weight that changes value with each collision due to absorption suppression, and may also be altered due to Russian roulette, splitting, or other variance reduction techniques. Each of the tallies in Section 7-3 must be appropriately modified to take the weights into account. If w_{ni} is the weight of the nth particle after the ith collision, then the contribution to the nth history is given by Eq. 7-142. With the path length estimator, for example,

$$w_n l_n = w_{n0} l_{n0} + w_{n1} l_{n1} + \cdots \tag{7-169}$$

where l_{ni} is the path length through the volume $\tilde{V}$ after the ith collision of the nth history. The sample mean and variance are then obtained from Eqs. 7-136 and 7-139. Hence for the path length estimator,

$$\phi = \frac{1}{\tilde{V}N} \sum_n w_n l_n, \tag{7-170}$$

$$S^2 = \frac{N}{N-1}\left(\widehat{\phi^2} - \widehat{\phi}^2\right), \tag{7-171}$$

$$\widehat{\phi^2} = \frac{1}{\tilde{V}^2 N} \sum_n (w_n l_n)^2. \tag{7-172}$$

The treatment of the surface crossing estimators is completely analogous.

The tallying for the collision estimator must be modified for the energy dependence of the cross sections as well as for the nonanalog tracking. To generalize Eq. 7-51 each collision must be weighted by $w_{ni}/\bar{\sigma}(E_{ni})$, where E_{ni} is the energy of the nth history particle before the ith collision. Equation 7-51 is then generalized to

$$\hat{\phi} = \frac{1}{\tilde{V}} \frac{1}{N} \sum_n \sum_i \frac{w_{ni}}{\bar{\sigma}(E_{ni})}, \tag{7-173}$$

where again only collision within $\tilde{V}$ for which E_{ni} lies within the energy interval included in Eq. 7-168 are tallied.

The tallies discussed thus far require that the flux be averaged over some volume $\tilde{V}$, or surface $\tilde{A}$. A difficulty presents itself if one is required to obtain the flux averaged over a very small volume, or worse, at a point. For a finite number of histories the variance of the result will rise rapidly as the volume decreases, since few if any of the particles will collide or even pass through the volume. Ultimately, the results will become totally unreliable as one approaches the point limit, since for a given number of histories N the most likely result will be that no particles contribute to the tally.

To circumvent this impass either the adjoint procedure alluded to in Section 7-6 must be applied, or alternately one of the flux-at-a-point tallies may be used.[2-6,15,16] The simplest of these tallies is the analog next-event estimator. In this approach each time a particle is born or undergoes a scattering collision the probability that a particle will be emitted in the direction $\hat{\Omega}'$ pointed toward the detector point is calculated. If this probability is multiplied by the probability that the particle will survive to the detector without making another collision, then an estimate of the point flux contribution can be made. Note that the tracking is not altered to actually direct a particle toward the detector; rather only the probability of the next event occurring at the detector is estimated before proceeding with the unperturbed tracking of the particle. This tally technique can be expensive since it involves the following calculation at each source particle or scattering site.

Consider the flux at a point contribution from a scattered particle. Let $f(\hat{\Omega} \cdot \hat{\Omega}'|E)\, d\Omega'$ be the probability in the laboratory system that a particle will be emitted in the solid angle $d\Omega'$ about the direction $\hat{\Omega}'$ pointed from the collision site toward the detector point. If $\vec{r}$ is the point of collision and $\vec{r}'$ the detector point, then

$$f(\hat{\Omega} \cdot \hat{\Omega}'|E)\, d\Omega' \exp\{-\tau(\vec{r}, \vec{r}', E')\} \tag{7-174}$$

is the probability that the particle will scatter into $d\Omega'$ and arrive at the detector point without further collision. Here $\tau(\vec{r}, \vec{r}', E')$ is the optical path length between $\vec{r}$ and $\vec{r}'$ for particles of energy E', the latter energy being determined from the scattering law.

To obtain the flux estimator we first write

$$d\Omega' = \frac{dA}{4\pi|\vec{r} - \vec{r}'|^2}, \tag{7-175}$$

where dA is an incremental area normal to the scattering line $\hat{\Omega}'$, and passing through the detector. Hence

$$f(\hat{\Omega} \cdot \hat{\Omega}'|E)\, dA \frac{\exp\{-\tau(\vec{r}, \vec{r}', E')\}}{4\pi|\vec{r} - \vec{r}'|^2} \tag{7-176}$$

is the probability of scattering toward the detector and passing through an incremental area dA normal to the line of flight at the detector. Since the scalar flux contribution may be defined as the number of particles passing through a unit area normal to the line of flight, the contribution from the scattering event at $\vec{r}$ is

$$d_{ni} = f(\hat{\Omega} \cdot \hat{\Omega}'|E) \left. \frac{\exp\{-\tau(\vec{r}, \vec{r}', E')\}}{4\pi|\vec{r} - \vec{r}'|^2} \right|_{ni}, \tag{7-177}$$

where the subscripts have been added to denote the ith collision of the nth history. Then the scalar flux at $\vec{r}$ is estimated from

$$\phi(\vec{r}') = \frac{1}{N} \sum_n \sum_i w_{ni} d_{ni}, \tag{7-178}$$

where w_{ni} is the particle weight.

In addition to the elaborate calculation that must be carried out at each tally point, there is a more fundamental problem with this estimator. Due to the $|\vec{r} - \vec{r}'|^2$ in the denominator, the variance does not exist if the point is in a scattering medium. Thus while the estimator can be used with the conventional variance estimates in vacuum or absorber regions, in a scattering region a collision at $\vec{r}'$ would cause an infinite flux contribution. As a result one of the more subtle flux-at-a-point estimators is required to correct this effect. Such estimators, however, tend to increase further the computation effort required for each contribution to the tally.

Geometrical Tracking

Heretofore we implicitly assumed that the problem domain consists of only one region, or at least that we knew how to select the region of the next collision. In fact the geometrical tracking of particles across material interfaces is often one of the most complex and time-consuming parts of a Monte Carlo calculation. It consists of the closely related tasks of mathematically specifying—and checking—the geometrical configuration of the problem, and of tracking particles across the resulting interfaces. In the following discussion we briefly outline the techniques that are used in specifying geometry and then describe a typical procedure of particle tracking.[7, 26]

Geometry Specification. Typically a Monte Carlo calculation will consider a problem spatial domain to be divided into a number of elementary regions

—sometimes called cells. Each such region has a specified composition of nuclides and is bounded by surfaces that are most often determined by first- or second-degree algebraic equations in a Cartesian coordinate system. Fourth-degree surfaces, such as in the case of toroids, are also frequently used.

Each interface or boundary in the problem thus can be represented by an equation, say

$$f_X(x, y, z) = 0. \tag{7-179}$$

The equation thus divides the three-dimensional domain of the problem into two domains. We designate as the domain X that part of space for which

$$f_X(x, y, z) \le 0, \tag{7-180}$$

while the domain $\bar{X}$, or not X, is that part of space for which

$$f_X(x, y, z) > 0. \tag{7-181}$$

With the foregoing formalism we can specify finite regions of space as the intersection of these subdomains. Suppose, for example, we want to have a finite cylinder of length H and radius R, centered at the origin and parallel to the z axis. Then let

$$f_A(x, y, z) = z - \frac{H}{2}, \qquad f_B(x, y, z) = z + \frac{H}{2},$$

$$\text{and} \qquad f_C(x, y, z) = x^2 + y^2 - R^2. \tag{7-182}$$

The cylinder designated as region D would then be

$$D = A \cap \bar{B} \cap C. \tag{7-183}$$

In designating these elementary regions care must be taken that the volume of the cell always lies on the same side of a boundary surface. An elementary region as shown in Fig. 7-10a, for example, would not be allowed because part of the cell lies on either side of the boundary surface $x - y = 0$. Such a cell would be divided into three elementary cells as indicated in Fig. 7-10b. The reasons for the foregoing restriction as well as the following piece of information will become clear as the tracking procedure is discussed.

After specifying the surfaces whose intersections form the elementary region, the regions that lie on the opposite side of each interface must also

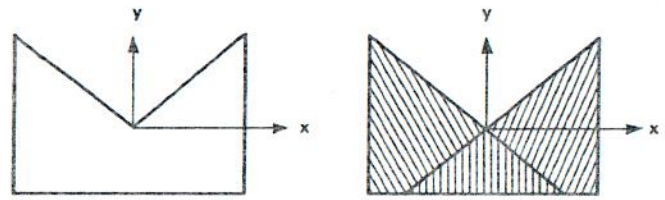

Figure 7-10 Elementary cells: (*a*) not permitted; (*b*) permitted.

be specified. Surfaces that form the outer boundary of the problem must be specified as vacuum, reflective, surface source, or other boundary conditions.

Tracking. In a Monte Carlo calculation the foregoing geometrical information is typically used in the following way. At the time a particle is born or at the time it makes a collision the elementary region that it is in and its x, y, z coordinates are known. Sampling is then carried out to determine the number of mean free paths the particle will travel before its next collision. From the previous sampling of the source distribution or the scattering kernel its direction cosines are also known. From this information the distance along the line of travel to each of the cell surfaces is determined. The distances that correspond to travel in the $-\hat{\Omega}$ direction are deleted, and the shortest distance in the $+\hat{\Omega}$ direction is designated as the distance to the region boundary. For example, in Fig. 7-11 u_3 is the distance to the boundary. This distance is computed in mean free paths (e.g., $u\sigma_t$) and compared to the number of mean free paths that the particle is to travel before its next collision. If the optical distance to the boundary is greater, then the next collision is in the same region, and its location can be determined. If the optical distance to the cell boundary is smaller than that to the next collision, the particle is determined to enter whatever region is designated to lie on the other side of the interface. Using the same procedure the optical distance along the flight path to the boundary of the newly entered cell is calculated. The sum of the optical paths traveled by the particle is then determined to decide whether it should collide in the region. If so, a collision point is determined. If not, the procedure is repeated for the next region that the particle enters, and so on, until a collision is made or the particle escapes the system.

This latter procedure for boundary crossing is illustrated in Fig. 7-12. Suppose that τ is the optical distance determined from the random number

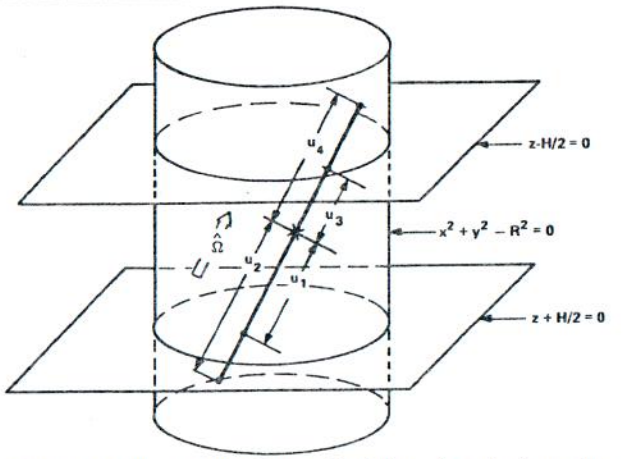

Figure 7-11 Example of Monte Carlo tracking in three-dimensional geometry.

to be traveled by a particle. The track begins in the region with $\sigma = \sigma_1$, as shown, and travels distances u_1, u_2, and u_3 in regions with cross sections σ_1, σ_2, and σ_3. If it is found that $\sigma_1 u_1 < \tau, \sigma_1 u_1 + \sigma_2 u_2 < \tau, \sigma_1 u_1 + \sigma_2 u_2 + \sigma_3 u_3 > \tau$, the particle would make a collision in region 3 after traveling a distance $u < u_3$ determined from

$$\sigma_1 u_1 + \sigma_2 u_2 + \sigma_3 u = \tau. \tag{7-184}$$

In practice a great deal more checking must go on during the tracking procedure. At each region crossing a check must be made to determine

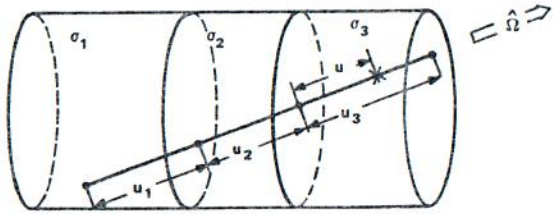

Figure 7-12 Illustration of boundary crossing for three-dimensional geometry.

whether a path length estimator of the flux is to be made for that region, just as a check must be made for the collision estimator each time a collision is made. Similarly, each boundary crossing may involve a current or flux estimator tally, and possible particle splitting or Russian roulette.

Description Simplifications. From the foregoing it is seen that the preparation of input for a Monte Carlo code with a complex geometry may be very complex. Indeed a great deal of cross-checking is necessary to avoid the all-too-common problem of specifying a logically inconsistent geometry with undefined or inconsistently defined regions of space. A great deal has been done both to simplify the specification of geometry and to provide internal consistency checks by the computer on geometrical data.

Although the detailed tracking must be done in terms of elementary volumes with no concave corners, material regions and/or regions over which one may want to tally volume-averaged fluxes or other quantities may have larger and more general shapes. These regions can be specified as the unions of the elemental regions heretofore discussed, since it is only they and not the elemental regions over which the results of the calculation are tallied. A great deal more can be done in reducing the amount of effort required to specify geometry. In combinatorial geometry methods[25-26] one is not asked to deal specifically with the equations for the surfaces. Rather, regions are specified in terms of elemental shapes, parallelepipeds, cones, spheres, and so on. A minimum of data on their size, shape, location, and orientation then needs to be provided. Such methods when combined with computer graphics techniques for picturing the geometrical results have come a long way toward making Monte Carlo methods accessible with a minimum amount of input, and reduced the chances for undetected input errors.

7-8 CRITICALITY CALCULATIONS

Thus far our discussion has centered about the Monte Carlo simulation of fixed source problems, governed either by the continuous form of the transport equation given by the time-independent form of Eq. 1-79 or its multigroup approximation. These forms of the equation are directly applicable to a variety of shielding and other types of problems. In reactor calculations, however, the fission process must enter the calculations. In reactor shielding problems it is most often incorporated into a fixed source problem as follows. A reactor criticality calculation is carried out—perhaps using a deterministic method—to determine the reactor power distribution. This distribution is then used as input data to the Monte Carlo shielding

calculation, by generating a fission spectrum source of neutrons that has a spatial distribution that is proportional to the power distribution. The entire calculation is then normalized to the reactor power.

At other times it is desirable to actually determine the system multiplication and integral information about power and/or flux distribution directly from a Monte Carlo calculation.[5,27-30] If this is to be done, more than one generation of neutrons must be considered, for the method of calculating k_{eff} closely parallels the outer iterations procedure discussed in conjunction with deterministic methods in Chapter 2.

Estimation of Multiplication

The basic idea used in calculations for the eigenvalue k is the same as that used in the inverse power iteration method. Given a distribution of fission neutrons, follow them through their lifetime and determine how many fission neutrons they give rise to in the next generation. The ratio of the number of fission neutrons in the jth generation, say F_j, to that in the $j-1$ generation then gives the multiplication of the system k_j for the jth generation. Hence

$$k_j = \frac{F_j}{F_{j-1}}. \tag{7-185}$$

After a sufficient number of generations the spatial distribution of neutrons from one generation to the next will become stationary except for statistical fluctuations. At this point the so-called fundamental mode or eigenfunction has been obtained, and the corresponding eigenvalue will no longer change from generation to generation. The converged solution for k has thus been obtained.

In a Monte Carlo eigenvalue calculation some finite number of neutron histories, say N, is originated by sampling a probability distribution of fission neutrons. This distribution is isotropic and is distributed in energy according to a standard fission spectrum $\chi(E)$. In the first generation the spatial distribution of the fission neutrons is determined either from a guess or as the result of a simplified calculation. The source for each succeeding generation is then determined from the results of the preceding generation.

In the jth generation each history is followed and its contribution, say $x_n|_j$, to the number of fission neutrons produced in the $(j+1)$ generation is calculated. The mean value

$$\hat{x}|_j = \frac{1}{N}\sum_n x_n|_j \tag{7-186}$$

may then be used as an estimate for k_j, since $\hat{x}|_j$ has in effect been normalized to one neutron in the preceding generation. From the history additional information must be obtained: the distribution of fission locations from which to start the next generation of particles.

In general, then, each generation of particle simulation proceeds in the same manner as in a fixed source problem with the exception that efficient tallies must be included (a) to specify the spatial fission distribution for the next generation, and (b) to estimate the number of fission neutrons produced in the next generation. In a strictly analog treatment of the within-generation problem these two things may be closely linked. In practice the two functions are often separate to optimize each.

In a strictly analog procedure absorption is not suppressed, and each particle has a weight of 1 until it is absorbed or escapes. At the time of absorption the particle will produce

$$x_n = \left.\frac{\nu\sigma_f(\vec{r}, E)}{\sigma_a(\vec{r}, E)}\right|_n \tag{7-187}$$

neutrons in the next generation. Here E and $\vec{r}$ designate the phase-space point of the particle absorption, where the cross sections are summed over all the nuclides present at $\vec{r}$. The value of $\vec{r}$ is recorded, and x_n particles are produced from an isotropic sampling of the fission spectrum. Since x_n is not an integer, the source particles would carry weights. This is avoided by writing

$$x_n = I_n + R_n \tag{7-188}$$

where I_n is an integer and $0 < R_n < 1$ is the remainder. One then starts I_n particles at $\vec{r}$. Then a random number ξ is generated and if $\xi < R_n$ an additional particle is generated. If not, then no additional particles are generated. In this way an unbiased estimate of x_n is obtained.

If more general nonanalog procedures are allowed, collision and track length estimators as well as the absorption estimator may be used to estimate the fission source distribution for the next generation. Both collision and track length estimators may also be used for the number of neutrons produced in the next generation. In general each neutron in a nonanalog simulation will carry a weight that is reduced at each collision to compensate for suppression of absorption. Thus the x_n in Eq. 7-187 will now be determined by

$$x_n = \sum_i w_{ni} c_{ni} \tag{7-189}$$

where w_{ni} is the weight of the neutron at the time of the ith event of the nth history that contributes to $\bar{x}$. The collision estimator is then

$$c_{ni} = \left.\frac{\nu\sigma_f(\vec{r}, E)}{\sigma_t(\vec{r}, E)}\right|_i, \tag{7-190}$$

where $\vec{r}, E$ is again the phase space location of the ith collision, and the cross sections are averaged over the nuclides present. The spatial location of the new source neutrons is calculated as follows.[7] Write

$$w_{ni} c_{ni} = I_{ni} + R_{ni}, \tag{7-191}$$

where again I_{ni} is an integer and the remainder has the property $0 < R_{ni} < 1$. Hence as with the collision estimator, we generate I_{ni} particles at $\vec{r}$ in an isotropic fission spectrum, and generate $I_{ni} + 1$ only if $R_{ni} > \xi$, where ξ is a uniformly distributed random number between zero and one.

Note that with either the analog absorption or the collision estimator one could generate one particle with a weight of x_n for absorption (or $w_{ni} x_{ni}$ for collision) at each specified space point. This could have the following deleterious effect. For absorption the number of particles per generation would decrease since the number of absorptions is smaller than the number of source particles, due to the surface leakage. Moreover, if leakage is significant, this reduction would be so rapid it would cause N to become unacceptably small before a fundamental mode distribution is reached. Likewise, if the collision operator is used, and one source particle per collision with a weight $w_n x_{ni}$, the result will be that with each generation the number of source particles will have very small weights. Thus after a few generations the number of particles would become exceedingly large. As a rule, it is desirable to keep the number of particles in each generation about the same. This is done exactly by the unweighted absorption and collision estimators if the x_n or x_{ni} are divided by the current estimate of k before Eq. 7-188 or 7-191 is applied.

Track length estimators are not well suited to determining the spatial distribution of fission for the next generation because they are not localized at specific space points. Track lengths, however, can provide a second and often almost independent estimate of the number of fission neutrons produced. Therefore, while the collision and path length estimators are always correlated to some degree, the variance of the multiplication estimate can be reduced by averaging the estimators. The track length estimator is simply

$$x_n = \sum_i w_{ni} l_{ni} \left.\frac{\nu\sigma_f}{\sigma_t}\right|_i \tag{7-192}$$

where w_{ni} is the neutron weight as it crosses region i, l_{ni} is its total track length across region i, and $\nu\sigma_f/\sigma_t|_i$ is the macroscopic cross section in region i.

Error Evaluations

While the foregoing computational algorithms take the form of straightforward generalization of those used for fixed source problems, the estimate of confidence intervals for Monte Carlo eigenvalues is fraught with difficulties not found in fixed source problems.[27,30] These arise from the interactions of two sources of error that appear in criticality calculations: (1) the finite number of histories N per neutron generation, and (2) the finite number of generations that are tracked before the calculation is terminated. Moreover, there is a tradeoff between these limitations. If a large number of histories per generation is followed, one may not be able to afford many generations. Conversely, if a large number of generations is required, severe limitation may be placed on the number of histories that can be tracked per generation.

It is difficult to determine a priori for a particular class of problems what combination of generations and histories per generation will give the most accurate result for a fixed amount of computing effort. Nevertheless, it is instructive to examine the limitation due to each of these parameters if those from the other were to be eliminated. Suppose first that a calculation with a very large number of histories per generation is carried out, the variance in the estimators $\hat{x}|_j$ for each generation is very small and might be sketched as in Fig. 7-13*a*. There is, however, a systematic bias which results from the fact that a fundamental mode distribution of fission neutrons is not used to obtain the first generation of neutrons; moreover, it is not reached after the relatively few generations that can be afforded.

Suppose, conversely, that a relatively small number of histories is tracked per generation in order to be able to track many generations. Now the difficulty is of a different nature. For even if it is assumed that enough neutron generations are tracked that the spatial sampling for the fission source will provide an unbiased representation of the fundamental mode, large variance will arise in the fission neutron estimators $\hat{x}$, due to the small value of N. The results are then likely to look similar to those in Fig. 7-13*b*, with the estimator having unacceptably large fluctuations about the true value; moreover, the magnitude of these fluctuations will not decrease, no matter how many generations are tracked.

As illustrated in Fig. 7-13, the error bars in the k_j results take into account only the statistical uncertainty for each generation, assuming that the exact fission source has been sampled, for they are calculated from the

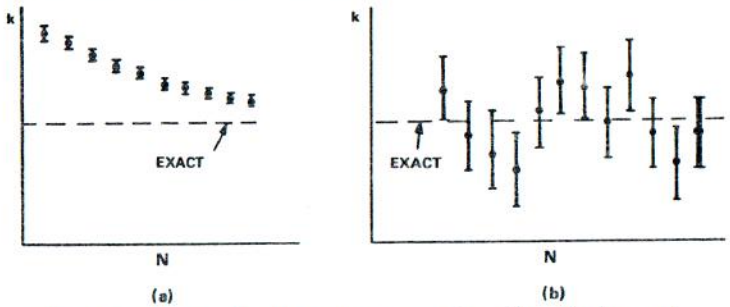

Figure 7-13 Variance of the estimators for a K eigenvalue problem: (*a*) a large number of histories / after few generations and (*b*) a small number of histories / after many generations.

variance $\sigma^2(\hat{x}|_j)$. Hence they give no indication of the lack of convergence indicated by Fig. 7-13*a*. Thus in practice one must be exceedingly careful not to begin using estimators of k_j until it is assured that the fission source distribution represents the fundamental mode. Usually it is possible to use the results from a similar problem or from a simplified deterministic calculation to obtain an initial guess that will greatly reduce the number of generations needed to reach a fundamental mode distribution.

Assuming that enough generations are followed to reach the fundamental mode, it usually is not possible to track enough histories N per generation to obtain an acceptably small value of the variance $\sigma(\hat{x}|_j) = \sigma^2(x|_j)/N$. To circumvent this difficulty one invariably averages values of $\hat{x}_j$ over a number of generations and calculates the multiplication from

$$k = \frac{1}{J}\sum_j \hat{x}|_j \tag{7-193}$$

where J is taken between some initial value J_0 large enough for the fundamental mode to have been reached and the final value $J_0 + J$ at which the calculation is terminated.

This generation-averaged multiplication will be more accurate than if the result of just a single generation were to be used. Most often the associated uncertainty is calculated from the variance for JN histories:

$$\frac{1}{J}\sum_j \sigma^2(\hat{x}|_j) = \frac{\sigma^2(x)}{JN}. \tag{7-194}$$

It should be realized, however, that this will underestimate the uncertainty in the result, even though a fundamental mode has been reached. The histories of successive generations are always correlated to some degree, since the fission neutron source points are determined by the collision or absorption points of neutrons of the preceding generation. Since the histories of successive generations are not totally independent, the derivation applicable to Eq. 7-194 found in Section 7-4 is no longer valid.

Although Eq. 7-194 rests on shaky foundations, in practice it is often found to yield acceptable error estimates. More general strategies may also be applied. For example, it may be desirable to increase the number of histories monotonically with each generation. By doing this the calculation may be shown to be a "fair game" that will converge to the exact result as the number of generations goes to infinity.[27]

REFERENCES

1. J. M. Hammersley and D. C. Handscomb, *Monte Carlo Methods*, Methuen, London, 1964.
2. J. Spanier and E. M. Gelbard, *Monte Carlo Principles and Neutron Transport Problems*, Addison-Wesley, Reading, Mass., 1969.
3. G. Goertzel and M. H. Kalos, "Monte Carlo Methods in Transport Problems," *Progress in Nuclear Energy II*, Series 1, Physics and Mathematics, D. J. Hughes, J. E. Sanders, J. Horowitz (eds.), Pergamon Press, New York, 1958, pp. 315–369.
4. M. H. Kalos, "Monte Carlo Methods," Lecture Notes, Ecole D'ete D'Analysis Numerique le Breau sans-Nappe, France, June–July 1981.
5. L. L. Carter and E. D. Cashwell, *Particle Transport Simulation with the Monte Carlo Method*, *TID-26607*, U.S. Energy Research and Development Agency Report (1975).
6. M. B. Emmett, "The MORSE Monte Carlo Radiation Transport System," *ORNL-4972*, Oak Ridge National Laboratory (1975).
7. Los Alamos Monte Carlo Group, "NCNP—A General Monte Carlo Code for Neutron and Photon Transport," Los Alamos Scientific Laboratory (1981).
8. R. N. Blomquist, R. M. Lell and E. M. Gelbard, "VIM—A Continuous Energy Monte Carlo Code at ANL," *Proc. Seminar-Workshop on the Theory and Application of Monte Carlo Method* April 21–23, 1980, *ORNL/RSIC-44*, Oak Ridge National Laboratory (1980).
9. N. F. Landers and L. M. Petrie, "KENO V—The Newest KENO Monte Carlo Criticality Program," *Proc. Seminar-Workshop on the Theory and Application of Monte Carlo Method* April 21–23, 1980, *ORNL/RSIC-44*, Oak Ridge National Laboratory (1980).
10. E. S. Troubetzkoy and H. A. Steinberg, "Monte Carlo Methodology as Implemented in SAM-F," *Proc. Seminar-Workshop on the Theory and Application of Monte Carlo Method* April 21–23, 1980, *ORNL/RSIC-44*, Oak Ridge National Laboratory (1980).
11. T. E. Hall and A. R. Dobell, "Random Number Generators," *SIAM Rev.* **4**, 230 (1962).

12. J. E. Freund and R. E. Walpole, *Mathematical Statistics*, 3rd ed., Prentice-Hall, Englewood Cliffs, N.J., 1980.
13. R. R. Coveyou, V. R. Cain, and K. J. Yost, "Adjoint and Importance in Monte Carlo Application," *Nucl. Sci. Eng.* **27**, 219 (1967).
14. D. B. MacMillan, "Comparison of Statistical Estimators for Neutron Monte Carlo Calculations," *Nucl. Sci. Eng.* **26**, 366 (1966).
15. M. H. Kalos, "On the Estimation of Flux at a Point by Monte Carlo," *Nucl. Sci. Eng.* **16**, 111 (1963).
16. E. D. Cashwell and R. G. Schrandt, "Flux at a Point in MCNP," *Proc. Seminar-Workshop on the Theory and Application of Monte Carlo Method* April 21–23, 1980, *ORNL/RSIC-44*, Oak Ridge National Laboratory (1980).
17. E. E. Lewis, "A Generalization of the Dirac Chord Method to Include Charged-Particle Phenomena," *Nucl. Sci. Eng.* **25**, 350 (1966).
18. M. H. Kalos, "Importance Sampling in Monte Carlo Shielding Calculations," *Nucl. Sci. Eng.* **16**, 227 (1963).
19. J. S. Tang, P. N. Stevens, and T. J. Hoffman, "Methods of Monte Carlo Biasing Using Two-Dimensional Discrete Ordinates Adjoint Flux," *ORNL-TM-5454* Oak Ridge National Laboratory (1976).
20. R. C. Bending, "Direction-Dependent Exponential Biasing," Proc. of the NEACRP Meeting of a Monte Carlo Study Group, July 1–3, 1974, *ANL-75-2* Argonne National Laboratory (1975).
21. H. Goldstein, *Fundamental Aspects of Reactor Shielding*, Addison-Wesley, Reading, Mass., 1959.
22. H. Steinberg and R. Aronson, "Monte Carlo Calculations of Gamma Ray Penetration," Technical Research Group, Inc., *WADC-TR-59-771* (1960).
23. C. W. Maynard, "An Application of the Reciprocity Theorem to the Acceleration of Monte Carlo Calculations," *Trans. Am. Nucl. Soc.* **3** (1960).
24. G. I. Bell and S. Glasstone, *Nuclear Reactor Theory*, Van Nostrand Reinhold, New York, 1970.
25. W. E. Selph and C. W. Garrett, "Monte Carlo Methods for Radiation Transport," *Reactor Shielding for Nuclear Engineers*, N. M. Schaeffer (ed.), *TID-25951*, U.S. Atomic Energy Commission Office of Information Services (1973).
26. H. A. Steinberg and E. S. Troubetzkoy, "Geometry Modeling for SAM-CE Monte Carlo Calculations," *Proc. Seminar-Workshop on the Theory and Application of Monte Carlo Methods*, April 21–23, 1980, *ORNL/RSIC-44*, Oak Ridge National Laboratory (1980).
27. R. C. Gast and N. R. Candelore, "Monte Carlo Eigenfunctions Strategies and Uncertainties," *Proc. NEACP Meeting of a Monte Carlo Study Group*, July 1–3, 1974, *ANL-75-2*, Argonne National Laboratory (1975).
28. D. B. MacMillan, "Monte Carlo Confidence Limits for Iterated-Source Calculations," *Nucl. Sci. Eng.* **50**, 73 (1973).
29. J. G. Moore, "The Solution of Criticality Problems by Monte Carlo Methods," *Adv. Nucl. Sci. Tech.* **9**, 73 (1976).
30. E. M. Gelbard, "Unfinished Monte Carlo Business," *Proc. ANS/ENS Int. Meeting on Adv. in Mathematical Methods of Nuclear Engineering Problems*, Munich, Germany, April 27–29, 1981, European Nuclear Society (1981).